Synergetical use of analytical models and machine-learning for data transport abstraction in open optical networks

Results in Engineering 30 (2026) 110251

Contents lists available at ScienceDirect

Results in Engineering

journal homepage: www.sciencedirect.com/journal/results-in-engineering

Review article

Recent developments and innovations in solar chimney power technologies: A focus on the last two decades

Hossein Ebadi [a], Sepideh Maleki [b], Christopher George [b], Maryam Haghsheno [c], Seyed Sobhan Aleyasin [d], Laura Savoldi [a], Nima Fathi [b,c,d,*]

[a] MAHTEP Group, Dipartimento Energia "Galilo Ferraris" (DENERG), Politecnico di Torino, 10129 Turin, Italy
[b] Department of Ocean Engineering, Texas A&M University, College Station, TX 77843, USA
[c] J. Mike Walker '66 Mechanical Engineering Department, Texas A&M University, College Station, TX 77843, USA
[d] Marine Engineering Technology Department, Texas A&M University, Galveston, TX 77554, USA

ARTICLE INFO

Keywords:
Solar chimney power plant (SCPP)
Enhancement techniques
Hybrid designs
Thermal analysis

ABSTRACT

Solar chimneys are one of the concepts used for power generation from solar energy and are becoming more popular as they rely on lower temperature operations than those of concentrating solar power (CSP). Referring to some technological barriers such as high capital costs, large land requirements, and performance limitations, solar chimney power plants (SCPPs) are shifting from their primary design to being more adaptable to the current energy market. In this regard, this paper reviews the technological development of SCPPs from different aspects and provides extensive analyses of a wide range of performance enhancement techniques. A collection of the most important innovations and modifications proposed by previous works is presented through historical and recent developments. The methods discussed in this study broadly cover geometric modifications, turbine advancements, collector enhancements, hybrid solar designs, and integrations with other technologies such as thermal energy storage, desalination, geothermal, nuclear, and hydrogen power plants. In addition, detailed energy analyses of the SCPPs, along with the economic and environmental implications, are presented by introducing the main challenges and prospects to provide a better understanding of the current level of technical maturity of this technology. The development trend suggests that employing concentrating solar reflectors in the collector section of SCPPs is one of the relatively underexplored techniques that might shape future hybrid CSP-SCPPs. Moreover, integrating SCPPs with thermal storage or geothermal units can mitigate the intermittent nature of their power production, making them a more reliable solution for further deployment.

1. Introduction

Reducing greenhouse gas (CO_2) emissions is essential to mitigating the adverse impacts of global warming, which is progressively leading to significant climate change. The coal and natural gas power plants altogether contribute to about 33 % of the total greenhouse gas (GHG) emissions of the USA in 2018 [1]. In 2024, global GHG emissions were recorded at 41.6 Gt of CO_2 equivalents (CO_2e), with 38.1 % attributed to the power industry, followed by transport (20.7 %), industrial combustion (17 %), and other sectors [2]. The international community has identified the energy transition framework as a pathway to decarbonize the power sector, reducing energy-related CO_2 emissions to combat climate change. Utilizing sustainable and green energy sources can reduce dependence on fossil fuels, accelerating the transition to cleaner energy in power generation facilities. Based on the predictions provided in the Faster Transition Scenario, due to the sharp increase in the penetration of renewable technologies, a 65 % decrease in direct CO_2 emissions from end-use sectors is expected by 2050 [3]. According to the latest world energy data reported by IEA [4], the share of renewable energies in final energy consumption is expected to increase from 13 % in 2023 to ~ 20 % in 2030. Moreover, the consumption of fossil fuels has already decreased to 82 % of the primary energy use, compared to 85 % in 2016 [5]. Clean and renewable energy sources such as wind and solar energy are the main candidates to replace the conventional electricity generation power plants that burn coal and natural gas. In particular, solar photovoltaic (PV) technologies are projected to reach the highest levels of installed capacity, exceeding 14.5 TW worldwide by 2050, according to the simulations performed based on a Net-Zero Emissions Scenario [6]. However, according to the capacity growth model

* Corresponding author.
E-mail address: nfathi@tamu.edu (N. Fathi).

https://doi.org/10.1016/j.rineng.2026.110251
Received 23 December 2025; Received in revised form 14 March 2026; Accepted 23 March 2026
Available online 24 March 2026

Nomenclature

SCPP	Solar Chimney Power Plant, –
CSP	Concentrated Solar Power, –
PV	Photovoltaic, –
CSPP	Concentrated Solar Power Plant, –
GSCPP	Geothermal–Solar Chimney Power Plant, –
HSDCPP	Hybrid Solar Double-Chimney Power Plant, –
LCOE	Levelized Cost of Electricity, \$/kWh
PCM	Phase Change Material, –
H_t	Chimney (tower) height, m
R_t	Chimney (tower) radius, m
R_c	Collector radius, m
q	Captured solar radiation, W/m^2
T_o	Ambient temperature, K
ρ_o	Ambient air density, kg/m^3
β	Volume expansion coefficient, 1/K
c_p	Specific heat of air at constant pressure, J/kg·K
g	Gravitational acceleration, m/s^2
η	Efficiency (overall system or component), –
Δp_{tot}	Total pressure drop in system, Pa
Δp_{turb}	Pressure drop across turbine, Pa
Δp_{dyn}	Dynamic pressure loss (kinetic losses), Pa
$\dot{m}$	Air mass flow rate through turbine, kg/s
P	Turbine/electrical power output, W
η_{turb}	Turbine efficiency, –
Ra	Rayleigh number, –
k	Thermal conductivity of the material, W/m·K
E	Total energy (internal + kinetic), J
e	Internal energy per unit mass, J/kg
V	Flow velocity magnitude, m/s
τ_{ij}	Shear stress tensor component, N/m^2
f_i	Body force per unit mass in direction i, N/kg
K	Thermal conductivity constant in Fourier's law, W/m·K
c_v	Specific heat at constant volume, J/kg·K
AR	Chimney area ratio (exit/entrance), –
SOFC	Solid Oxide Fuel Cell, –
SOEC	Solid Oxide Electrolysis Cell, –

described in [7], the PV capacity is anticipated to reach almost 25 TW, compared to slightly more than 700 GW installed today. In the same study, concentrated solar power (CSP) technology shows a trend of stagnating progress and is expected to increase by six times, reaching a capacity of 6.4 GW (2021 data [8]). On the other hand, the IEA suggests more impressive progress for CSP, with almost 430 GW installed by 2050 in a Net-Zero Emissions Scenario.

In addition to its direct energy delivery, solar energy is the basis of most renewable energy sources. It appears in the form of stored energy such as wind (short-term storage) and biomass (long-term storage) [9]. Solar energy conversion to electricity and thermal power is also diverse and can be classified as shown in Fig. 1. One way to exploit this abundant energy for power generation purposes is the utilization of solar thermal power through different thermal processes, which can be divided into two main categories. The first one, operated in low-temperature conditions, involves harnessing the sun to produce pressure using an enclosed volume of air (solar chimney technology) or to make a constant temperature gradient in shallow brine ponds to run a small heat engine (solar ponds) [10]. In the second mode, only direct solar radiation is used, employing a reflector to concentrate the solar energy and produce the larger temperature gradient required for power generation in a conventional heat engine [11].

One of the main drawbacks of renewable energy plants is the variation and fluctuation of their power output, limiting their application for baseload power. This intermittency has affected the role of solar power technologies in the niche energy market, making them unreliable for continuous energy supply to the end-users [12]. However, among the nominated solar power technologies, the power generation concept is straightforward within a solar chimney power plant (SCPP). Energy from the sun not only warms up the air but also the ground under the collector. The stored energy in the ground heats up the air during periods of reduced solar radiation, making the power output of SCPPs more uniform during day and night. As a result, SCPPs are one of the rare renewable energy power plants that can produce sustainable output with minimal fluctuations, suitable for baseload power applications. The power generation process in solar towers requires a relatively small amount of water compared to other renewable sources, desirable for hot and dry locations suffering from long-term droughts, such as Central

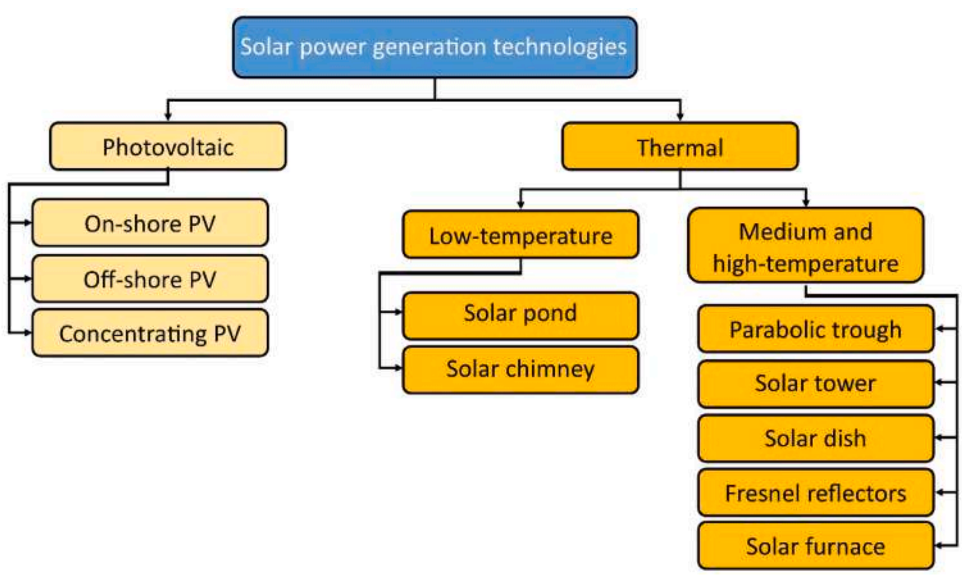

Fig. 1. Broad classification of solar power technologies.

Africa and the Middle East. Despite the unique advantages of SCPPs, their low efficiency in the order of 0.5–5 % [13,14] is the main drawback, limiting their attractiveness to investors compared with other renewable resources.

Research on SCPPs dates back to around 1970, preceding the construction of the first prototype in Spain. This plant operated between 1982 and 1989, and its electricity was used in the local electric network [15,16]. Several researchers studied the effect of different geometrical parameters on plant efficiency. Padki and Sherif [17], in 1999, stated that the converging top chimney could increase the power and efficiency of the SCPP. However, the mathematical model of Chitsomboom [18] revealed that converging the top did not improve the power and efficiency of the plant, and they remained almost constant. In 2000, Gannon and von Backström [19] applied a one-dimensional (1D) compressible flow model to calculate thermodynamic variables as a function of chimney height, wall friction, additional losses, internal drag, and area change. It was found that for a given chimney height, an increase in area ratio resulted in a higher pressure drop in the chimney, corresponding to a higher power output.

Schlaich [20] reported that according to his mathematical model, there are no optimal dimensions for a solar chimney. However, a thermo-economically optimal configuration for each plant might exist based on the construction costs. The numerical calculation performed by Pretorius and Kroger [21] in 2007 showed that the power of an SCPP depends on its collector roof shape as well as the inlet height. Also, the simulation performed by Maia et al. [22] concluded that the most important geometric dimensions are the height and diameter of the chimney. Zhou et al. [23] employed a theoretical model that was validated with the experimental results of the Manzanares prototype. They calculated the maximum chimney height to avoid negative buoyancy, as well as the optimal chimney height for maximum power output. It was found that both the maximum and optimal height increased with a larger collector radius. Overall, while some geometric modifications—such as the converging chimney configuration—have produced conflicting conclusions in the literature, most studies consistently agree that the principal design parameters governing SCPP performance are the chimney height, chimney diameter, and collector dimensions, which directly influence the pressure difference and buoyancy-driven airflow through the system. There has been ongoing research and investigations on solar chimneys in recent decades to find efficient and low-cost methods to increase their efficiency. In 2010, Zhou et al. [24] presented a thorough discussion on the state-of-the-art technologies used for SCPPs. A historical review of SCPPs including the cost modeling was later published by Al-Kayiem and Aja [25]. Kasaeian et al. [26] provided an updated review of the latest developments in the field of SCPPs, highlighting the gaps in experimental and numerical studies to propose a roadmap for future studies. Guo et al. [27] investigated the seven fundamental questions regarding the commercialization of SCPP technology to recognize the areas that need further development. A literature review was conducted by Omara et al. [28] on the integration of phase change materials (PCM) with SCPPs, indicating the material type and effects on the performance. Rashid et al. [29] focused on the integration of PCMs with solar chimneys, reviewing the applications from SCPPs to architectural building environments. Pradhan et al. [30] provided a list of design parameters with innovations used in SCPPs and addressed the environmental aspects of such technologies. An extensive review of the hybrid solar chimney was also reported by Ahmed et al. [31] to open a new window in this field for possible combinations between a solar chimney and other renewable or conventional energy systems. Das and Parvathy [32] conducted a critical review study on SCPPs, taking the operational and environmental factors into account for the estimation of carbon emission mitigation with the implementation of such technology. Other review works [33–35] found in the literature revolve around the latest findings resulting from innovative designs and enhancing techniques.

Recent review articles have significantly advanced the understanding of solar chimney power plants by examining different aspects of their development. For example, Zhu et al. [36] presented a comprehensive overview of SCPP technologies, discussing system components, performance characteristics, geometric configurations, hybrid concepts, and related economic and environmental considerations. Mandal et al. [37] reviewed hybrid solar chimney power plants with particular emphasis on multi-objective optimization approaches and the integration of artificial intelligence and machine learning techniques for system optimization. Similarly, Kassaei et al. [38] focused on experimental investigations of solar chimneys, categorizing experimental studies based on geometric parameters, materials, environmental conditions, and innovative configurations to identify research gaps in experimentally tested designs. Building on these recent contributions, the present review places particular emphasis on the engineering evolution of performance-enhancement approaches in SCPP systems. Specifically, it synthesizes how different modification strategies—such as geometrical changes, turbine developments, collector and absorber innovations, and cross-sector integrations—have been used to improve system performance and feasibility across the literature. By organizing the discussion around these enhancement pathways and linking them to techno-economic and environmental implications, this work provides a complementary perspective to existing reviews and highlights practical directions for future SCPP development and implementation.

2. Description of SCPP

A solar chimney power plant consists of three main parts: a solar collector, a turbine, and a chimney. In an SCPP, the energy of hot air is converted to electrical energy. The collector has a transparent roof to collect solar radiation and heat up the air underneath. At the center of the collector, a tower is located, and a turbine is typically installed at its base. Due to the buoyancy effect, the hot air flows up through the tower and passes through the turbine. In this process, the kinetic energy of the air is converted to electrical energy. A typical solar chimney is shown in Fig. 2 [39].

2.1. Solar collector

The solar collector is the section that provides the greenhouse effect to guide the air toward the chimney. As shown in Fig. 3, the solar collector comprises a large transparent roof, mounted on a metal matrix and supported by several columns, where the height of the roof has a slight increase in the radial direction toward the center, see Fig. 4. In principle, as the solar radiation reaches the transparent roof, a fraction of the beam and diffuse solar radiation is transmitted into the collector zone to be absorbed by the ground beneath the roof. As a result, the ground transfers the obtained heat to the air above, increasing the air temperature and driving it from the periphery toward the center, using buoyancy. In general, solar collectors cover a considerable area of land, and the choice of roof material significantly impacts the initial investment [40]. Glass and plastic materials are the two alternatives proposed in the literature, where using Low-Density Poly-Ethylene “LDPE” as the collector cover can improve economic efficiency. However, LDPE material can be degraded under prolonged exposure to high solar flux, which was investigated by Boualleg et al. [41]. Exploring the effects of natural aging on an LDPE film for a duration of 3 years, scientists found that with similar environmental constraints, the failure stress was reduced by 50 %, while collector transmittance also decreased proportionally, leading to a reduction in SCPP performance. Moreover, simulation results indicated that by increasing the initial dimensions by 23 %, the above-mentioned losses would be offset, reaching the target power production, and the optimum life cycle of the collector material would be 3 years. In another work, Pretorius and Kröger [42] realized that the selection of better glass material increased the annual power output of the systems by 3.4 %. Table 1 summarizes some of the important materials recommended for a solar collector in SCPPs.

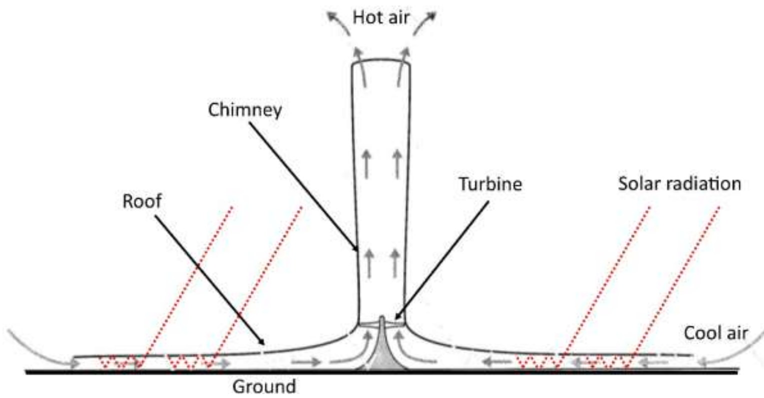

Fig. 2. Schematic of a typical solar chimney (adapted from [39]).

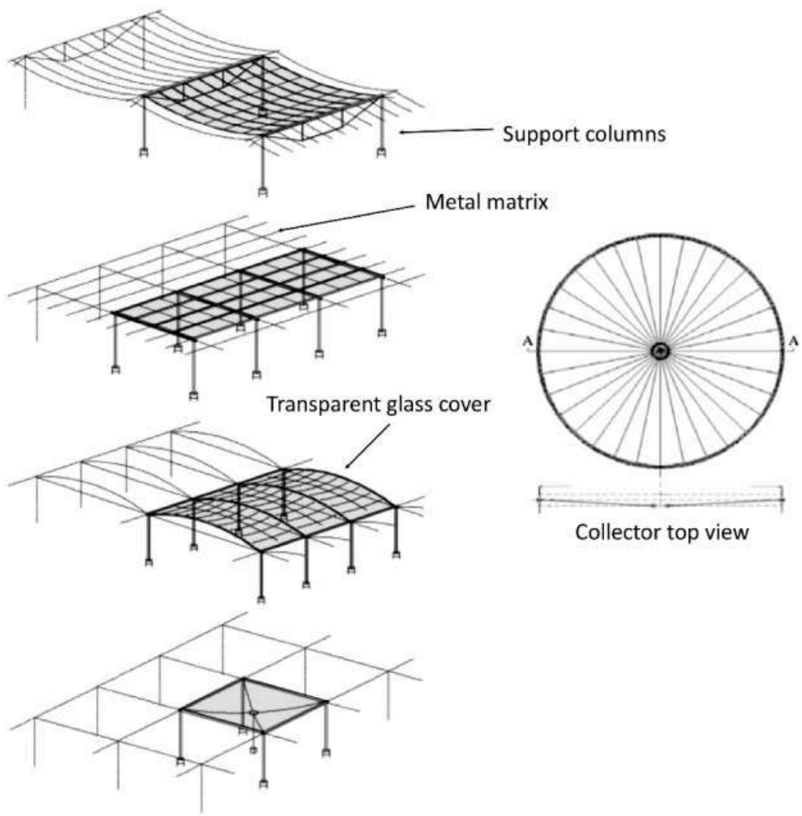

Fig. 3. The layout of the various collector structures, including the roof, matrix, and support frames (adapted from [40]).

2.2. Turbine

One or more wind turbines are used at the base of the solar chimney to convert the kinetic energy to electricity and transmit it with power electronics. To guide the airflow coming from the solar collector toward the turbine rotors, a knee-like section with some vanes is designed to redirect the flow from horizontal to vertical and consequently propel the generator. A diffuser can also be used after the turbine, which is located inside the solar chimney [25]. In addition to the basic design with a single vertical-axis turbine (Fig. 4a), two more common configurations have been introduced with multiple vertical axial turbines (Fig. 4b), and multiple horizontal-axis turbines (Fig. 4c) [43].

2.3. Chimney

The chimney, as the main component of the SCPP, is typically located at the center of the solar collector to conduct the heated air from the collector to the atmosphere. The temperature difference between the inside and outside of the chimney creates a buoyancy effect, leading to an air updraft flow through the tower. Although the vertical column has a large height, the friction loss is relatively low due to the large flow cross-section of the duct [44]. One of the important factors is the updraft velocity, which is a function of air temperature rising inside the collector and the pressure drop across the turbine. Diverging the chimney by decreasing the ratio of its entrance area over its exit area (AR) enhances the pressure difference, while the convergent shape helps to have a higher temperature within the collector [45]. According to Hu et al. [46], the optimum AR is also affected by the chimney height.

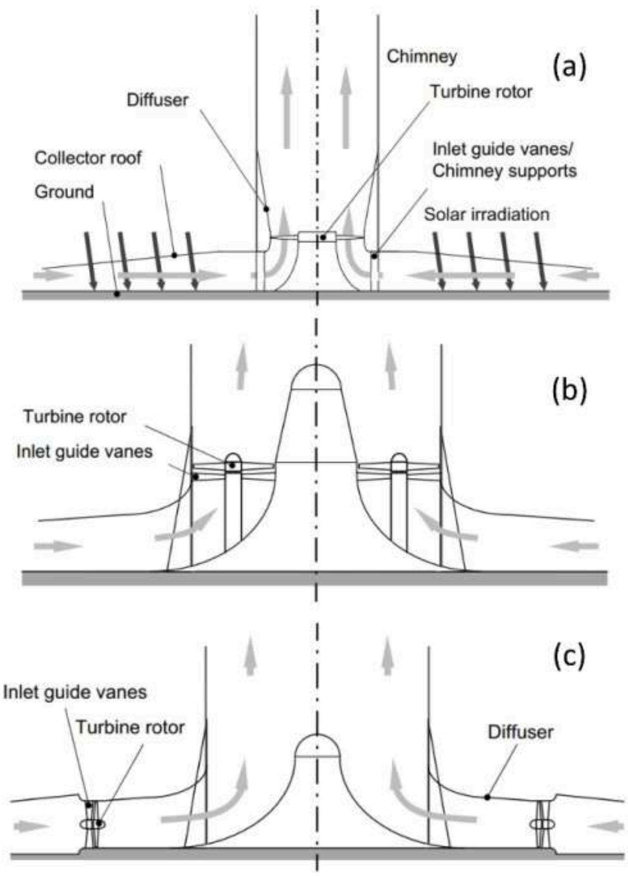

Fig. 4. Various configurations of turbine installation; (a) single vertical axis, (b) multiple vertical axis, (c) multiple horizontal axis [43].

Table 1
Materials for the solar collector cover in SCPP [181,182].

Material	Transmittance
Anti-refluxing glazed glass	0.85–0.9
Window glass	0.87
Greenhouse glass	0.85
Polycarbonate	0.844
Fiber glass reinforced polyester	0.831
Corrugated fiber glass	0.78–0.79

Furthermore, Hoseini et al. [47] concluded that diverging chimney configurations generate higher power output compared with horizontal and convergent designs. While sometimes, the upper two-thirds of the tower shell is constructed with a diverging conical shape to increase the aerodynamic performance [24], an optimization problem should be solved to find the optimum chimney and collector design. Several configurations for the collector and chimney are illustrated in Fig. 5.

According to Wang and Fan [48], the chimney is vulnerable to wind load, temperature stress, earthquakes, and construction defects. Balijepalli et al. [49] asserted that being weather-resistant, lightweight, strong in structure, withstanding wind, and overall loading conditions are among the selection criteria of the proper material for solar chimneys. Table 2 presents a list of materials suggested for solar chimneys.

3. Historical development and advancements

One of the earliest ideas about solar chimney power plants was introduced in 1903 by Cabanyes, a Spanish artillery colonel [50]. He suggested an air heating apparatus with a chimney attached to a house to generate electricity. A propeller was placed inside the chimney to extract electricity from the heated air. The proposal of constructing a Solar Aero-Electric Power Plant in North Africa was presented to the French Academy of Science by Professor Bernard Dubos in 1926. Since the slope of the mountain was considered as the construction site, he claimed that the air could reach a speed of 50 m/s. Therefore, a wind turbine at the top-end of the chimney could extract a huge amount of energy [51]. Building a prototype in 1982 in Manzanares, 150 km south of Madrid in Spain, can be considered as the first step in developing practical solar chimney power plants. The chimney height and diameter were 195 m and 10 m, respectively. The collector area was 46,000 m^2 and it produced 50 kW of electrical power. The construction of the prototype was commissioned by the Ministry of Research and Technology of the Federal Republic of Germany [15]. In 1984, Haff [16] published new test results from the Manzanares plant, including energy balances, collector efficiency, and pressure losses due to friction. The SCPP technology has high reliability due to a few moving parts, and it does not consume cooling water. The simplicity of the technology and materials used, along with the use of the ground as a natural heat storage, are among the additional advantages of SCPP [40]. Mullett [52], in 1987, started developing a theoretical model for SCPP by deriving overall efficiency and other performance data. He discovered that the SCPP concept was meaningfully productive only when built at very large scales. The study showed that efficiency is proportional to the chimney height, as given in Eq. (1):

$$\eta = \frac{gH_t}{c_p T_0} \tag{1}$$

where g is the gravitational acceleration (m/s^2), H_t is the chimney height (m), c_p is the air heat capacity $\left(\frac{J}{Kg.K}\right)$ and T_0 is the ambient temperature. Padki and Sherif [53], in 1989, used the result from the Manzanares prototype to extrapolate medium to large-scale models for SCPPs. In 1991, Yan et al. [54] developed a detailed model for SCPPs by using practical correlations. They introduced some equations, including air velocity, air flow rate, output power, and thermo-fluid efficiency. The research was followed by another numerical model in 1992 by Padki and Sherif [55].

Bernardes et al. [56], in 1999, submitted the first CFD solution of the flow inside the SCPP. They suggested a solution for the Navier-Stokes and energy equation for natural laminar steady-state flow and predicted its thermo-hydrodynamic behavior.

Kroger and Blaine [57], in 1999, investigated the influence of prevailing ambient conditions. The conclusion was that air moisture can increase the driving potential, though condensation might happen in some cases. In the same year, Kroger and Buys [58], developed mathematical relations to calculate differential pressure due to heat transfer correlations and friction for the radial flow between the roof and the collector. Padki and Sherif [17] continued developing equations for SCPPs and suggested a set of differential equations. They obtained expressions for the generated power and efficiency by considering some simplifications.

Gannon and von Backström [19], in 2000, analytically studied chimney friction, and analyzed different losses in the system, turbine, and exit kinetic energy for SCPPs. They employed a simple collector model to include the coupling equations of mass flow and temperature rise, and validated their results by comparing the simulation of a small-scale plant and experimental data, as illustrated in Fig. 6. The model can be used to predict the efficiency and operating range of large-scale plants. They assumed one-dimensional compressible flow and developed equations for thermodynamic variables as functions of chimney height, wall friction, additional losses, internal drag, and chimney area changes. The pressure drop due to the vertical acceleration of the air was three times greater than the pressure drop related to wall friction; however, the effect of vertical acceleration on the pressure drop can be mitigated by employing a flared chimney shape.

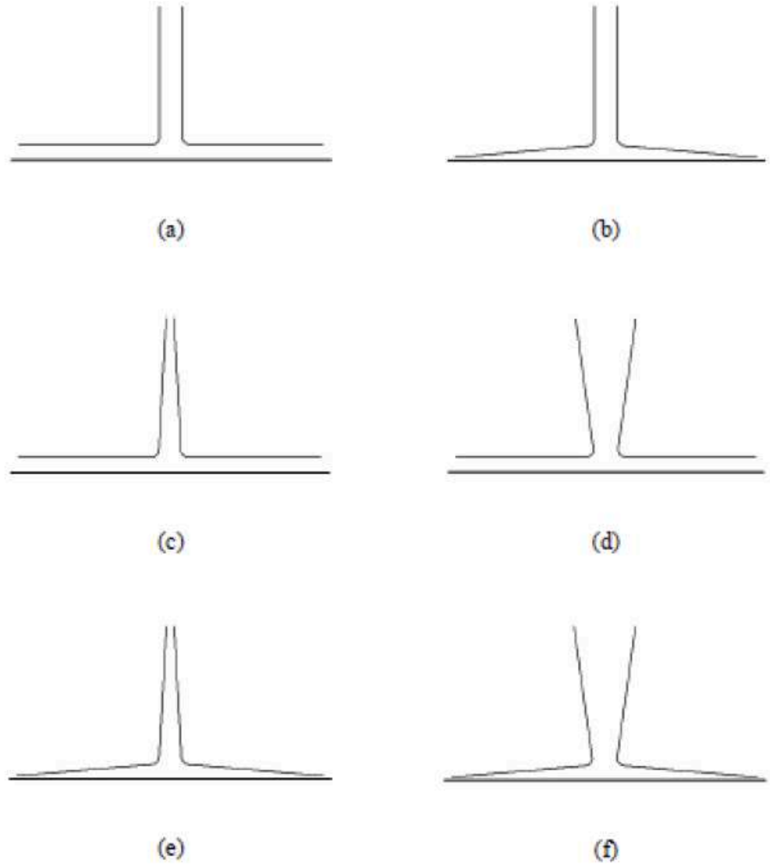

Fig. 5. Schematic of different collector and chimney configurations in a typical solar chimney tower [24].

Table 2
Possible materials for solar chimneys and their related properties [49].

Thermosetting plastic material	Glass transition temperature (°C)	Glass melting temperature (°C)	Thermal conductivity (W/m·K)	Density (kg/m^3)	Specific heat (kJ/kg·K)
Polyvinylchloride (rigid PVC)	87	212	0.14–0.28	1467	0.9
Nylon 6,6	100	265	0.24–0.3	1140	0.0017
Polycarbonate	150	265	0.19–0.22	1200	1.17
Polyester	73	265	-	1370	1.3–1.5
Polyethylene	-90	137	-	970	1.25
Polypropylene	-14	176	-	905	1.92
Poly tetra fluoroethylene	-90	327	0.25	2200	1.172

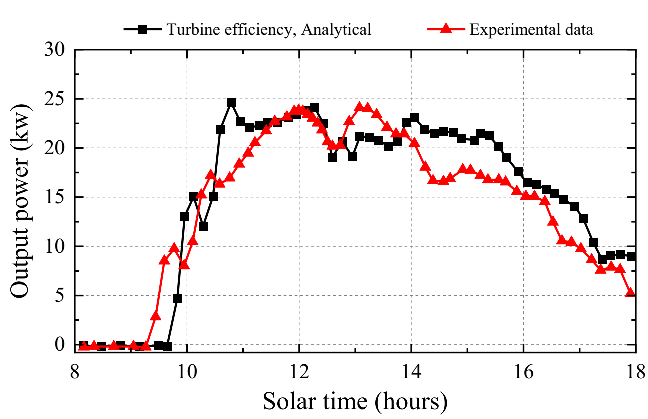

Fig. 6. Comparison between numerical results and experimental data from Manzanares [19].

Gannon and von Backström [59] extended their research in 2002 by examining the turbine's characteristics. They proposed a turbine design for a full-scale SCPP. Most of the turbine dimensions were obtained using a three-step design method and free vortex analysis. Also, the blade profile was optimized (minimum chord and low drag) using the scheme coupled to a surface vortex method. They claimed that the designed turbine can extract around 80 % of the flow energy. The experimental results of their designed turbine indicated a total-to-total efficiency of 85–90 % and a total-to-static efficiency of 77–80 % [60,61].

In 2003, Bernardes et al. [62] performed a comprehensive analysis using numerical methods to describe SCPPs' performance, including the output power, the effect of ambient conditions, and structural dimensions on the produced power. The model was validated with experimental data and used to predict the behavior of large-scale SCPPs. The height of the chimney, the pressure drop across the turbine, the diameter, and the optical properties of the collector were identified as significant factors in SCPPs.

Schlaich et al. [44,63], explained some functional principles of SCPPs and presented some information on designing, constructing, and operating the prototype in Manzanares. Also, technical and economic issues about future SCPPs were suggested for consideration.

In 2003, von Backström [64] developed an analytical method to calculate the pressure drop in very tall chimneys of SCPPs. Equations for vertical pressure and density distribution were presented as functions of Mach number, wall friction, and internal bracing drag.

In 2004, the influence of winds on SCPPs' performance was studied by Serag-Eldin [65]. The flow pattern near a small-scale SCPP was predicted employing computational methods, including partial differential equations for conservation of mass, energy, and momentum, and a two-equation turbulence model. The results from the numerical model showed a severe decline in power output in the case of strong or low-speed winds, except for low-height collectors.

Kirstein and von Backström [66], in 2006, published their experimental and CFD results. They studied the loss coefficient in the transit section between the chimney and turbine as a function of the collector's roof height and the inlet guide vane stagger angle. The numerical and experimental data showed significant agreement, validating the applicability of the model to predict the behaviors of full-scale SCPPs. Based on the results from the prototype in Manzanares, Ming et al. [67] performed a numerical study to modify the geometry in an attempt to achieve better performance. The effects of different factors on the performance of an SCPP were examined, and the results showed a reasonable agreement between the model and prototype.

Pretorius and Kroger [68,69] studied the performance of a large-scale SCPP. They chose a reference plant in South Africa and investigated the heat transfer and momentum equations. They claimed that 24-hour electricity production was possible, and the power was a function of the collector's roof shape and height. Also, the impacts of a more precise turbine inlet loss coefficient and different types of soil and roof glasses on the efficiency of the SCPP were investigated. Their findings exhibited that the amount of power output decreased significantly by employing the new heat transfer equation; however, using better-quality glass improved the performance. Modifying the turbine coefficient led to a very small increase in annual power plant production. According to their studies, the effect of using Limestone and Sandstone soil is the same as the original model using Granite.

Von Backström and Fluri [70] numerically examined the validity of the assumption that the optimum ratio of pressure drops in turbines to achieve the maximum power is 2/3 of the system's available pressure difference. It was concluded that this theory might overestimate the flow passage in the plant and design a turbine without sufficient stall margin.

Huang et al. [71] examined the effect of solar radiation on the performance of SCPPs. They used simulation and introduced the Boussinesq and Discrete Ordinate radiation model. Koonsrisuk and Chitsomboon [72] introduced the use of dimensionless variables and checked the validity of their model using computational fluid dynamics. In the same year, Ming et al. [67] introduced different models for heat transfer and flow in chimneys, collectors, and turbines. The models were validated against the experimental results of the Manzanares prototype.

4. Recent enhancements and innovations

There has been much analytical, experimental, and numerical work on the subject of SCPPs since the concept was introduced in the early 20th century. Due to high capital costs, especially for constructing tall chimneys, the solar tower power plant technology has not yet attracted commercial interest. There has been ongoing research and investigations on SCPPs in recent decades to increase efficiency and cost-effectiveness.

4.1. Geometrical modifications

Most enhancement work reported in the literature focused on modifications to the geometric parameters of SCPPs. Pasurmarthi and Sherif [73,74] conducted experimental and theoretical investigations on three different model-scale solar chimneys (see Fig. 7 and 8). They examined the effects of extending the collector base as well as an intermediate absorber on the efficiency of solar chimneys. Obtained experimental data and the theoretical model results showed that both modifications enhanced the solar chimney efficiency by increasing the hot air temperature and air mass flow rate.

Mehla et al. [75] optimized the power output of a pilot updraft solar tower by varying the chimney height and diameter. It was observed that a chimney with a diameter and height of 80 cm and 8 m, respectively, produced the maximum air velocity in the fixed collector diameter of 1.4 m. Najmi et al. [76] experimentally investigated the parameters affecting the power output of a model-scale solar tower. The plant had a 40 m x 40 m collector with a chimney height of 60 m and a diameter of 3 m. The authors suggested that using a collector with a height of 1.3 m and double-glazing glasses on the roof could increase the power output. Elsayed et al. [77] introduced various swirl guide blades into the collector of an SCPP, inspired by turbomachinery systems, as shown in Fig. 9. These configurations are differentiated based on available path length inside the collector, where each segment was obtained by two curved guide vanes, following an interpolation from different points of intersection with axes. Numerical investigations confirmed the positive effects of the curved vanes on the turbine performance, increasing the average velocity from 1.19 m/s (without guide vanes) to 2.56 m/s (eight curved vanes).

Ghalamchi et al. [78] studied the air temperature and velocity within a pilot solar chimney power plant with a collector diameter of 3 m and chimney height of 2 m (See Fig. 10). A maximum velocity of 1.3 m/s was reported with 26.3 °C temperature difference between the collector exit and the ambient air. The experimental data showed that the output power increased by reducing the collector inlet height (Table 3).

Mullett [52] developed one of the first one-dimensional analytical models to evaluate the efficiency of SCPPs with constant-diameter cylindrical shape chimneys. His model predicted that the efficiency of solar chimney plants is a function of chimney height, with a value of about 1 % for a height of 1000 m. Lodhi [79] analytically investigated the power output and efficiency of solar chimney plants. His analysis suggested that the power output is directly related to chimney height, and the theoretical peak efficiency of a solar chimney plant is in the range of 0.4–6 %. Dai et al. [80] investigated the effect of solar chimney height, the diameter of the collector, and the ambient air on an SCPP in China. Their mathematical model predicted an enhancement in the plant power capacity with the increase in chimney height and collector diameter. It was also claimed that the plant's power capacity was independent of the ambient air. The theoretical model based on the experimental data of the Manzanares prototype [15,16] predicted an optimum chimney height of 615 m to produce maximum power of 102.2 kW. The model also showed that the optimum chimney height increased with an increase in atmospheric lapse rate (temperature difference with increasing altitude).

Maia et al. [22] studied the unsteady flow within solar chimneys using numerical simulations. The obtained numerical results were compared with available experimental data. The results showed that the tower height and diameter are the two main parameters affecting efficiency. Okada et al. [81] numerically and experimentally studied the airflow within a diffuser chimney. The inner diameter of the proposed diffuser tower increased with its height; therefore, a low-pressure region was generated at the bottom of the tower. It was shown that a diffuser chimney induced up to 1.44 times higher air velocity than a conventional cylindrical chimney. The power output of an SCPP with a diffuser chimney was reported to be almost 3.0 times higher than that of conventional ones.

Das and Chandramohan [82] applied a 3D κ-ε turbulent CFD model to investigate the effect of geometrical parameters such as chimney height and collector roof angle on the efficiency of a solar updraft tower. It was shown that increasing the chimney height from 3 to 8 m raises the air temperature and its velocity (31 %) at the chimney base, leading to higher output power, as illustrated in Fig. 11 (produced from data

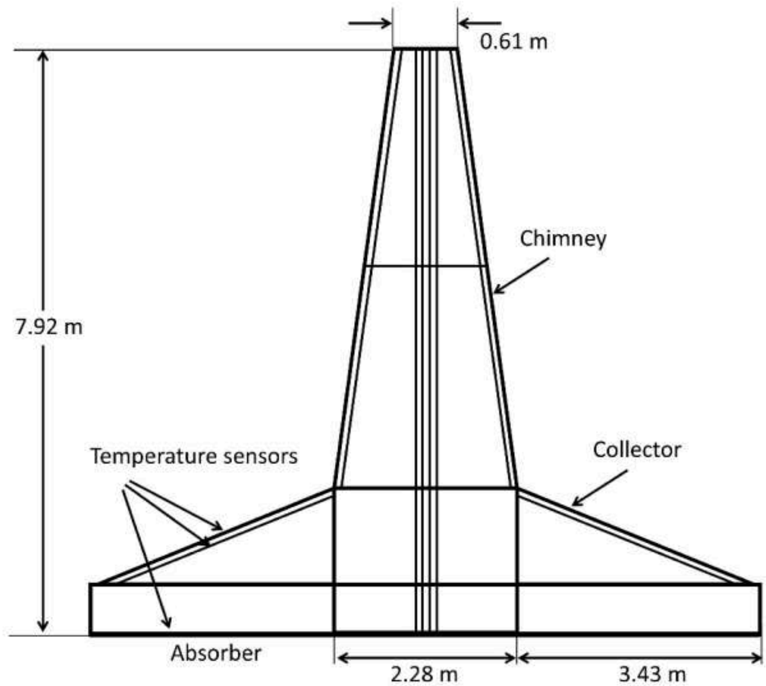

Fig. 7. Schematic of type I solar chimney used in the experiments (adapted from [73]).

reported by [82]).

Das and Chandramohan [82] also evaluated the effect of the collector roof angle on the system within a range of (20° – 35°) where the other parameters were fixed. It was observed that by increasing the collector roof angle, the flow velocity and mass flow rate increased while the pressure drop, collector efficiency and output power decreased (Fig. 12.)

Shirvan et al. [83] studied the effect of chimney height, diameter, and collector roof angle on the power output of a model-scale solar tower. Results from a 2D axisymmetric numerical simulation showed that the output power enhanced as the chimney height and diameter increased. Hassan et al. [84] utilized a 3D turbulent CFD model to investigate the effect of the chimney diverging angle and slope of the collector roof on the performance of the Manzanares prototype solar tower. For a typical case, the output power first increased by increasing the diverging angle from 0 to 1 and then decreased by further increasing the diverging angle. It was indicated that the increase in diverging angle by 1 degree raised the air velocity from 9.1 m/s to 11.6 m/s. Gholamalizadeh and Kim [85] conducted numerical simulations to study the effect of an inclined collector roof on the Manzanares prototype solar tower. Numerical results predicted an enhancement in mass flow rate within the chimney using an inclined roof collector. Numerical simulations were conducted in a large-scale solar tower with a chimney height of 1 Km and a collector diameter of 2.5 Km using a 2D axisymmetric model [86]. Numerical results showed that the power output increased by decreasing the collector top roof inclination angle. Increasing the heat flux on an inclined collector roof did not enhance the air velocity due to vortex formation near the collector inlet.

Koonsrisuk and Chitsomboon [87] used the CFD approach to investigate the effect of variation in the air flow area of the chimney and the collector on the performance of an SCPP. Results showed that static pressure, mass flow rate, and power output increased in a divergent chimney compared to a conventional cylindrical one. Moreover, an enhancement in static pressure was predicted in a collector with an inclined roof.

Inflatable solar towers have been proposed to replace conventional steel chimneys, reducing construction costs while better tolerating severe weather conditions. Putkaradze et al. [88] proposed a new design using an inflatable chimney consisting of a free-standing stack of hollow gas-filled tori (See Fig. 13). The authors proposed an optimum shape for their free-standing chimney, enabling it to withstand a force under hurricane-strength wind loads [89,90].

Papageorgiou et al. [91] proposed a floating solar chimney, as shown in Fig. 14, made of a reinforced fabric core and a set of BOPET/HDPE lifting tubes filled with lighter-than-air gas. BOPET rigid rings filled with compressed air were offered to support the integrity of the fabric core, while an accordion-like structure was used to attach the tower to the ground. The proposed design was shown to have an efficiency of 4–7 % with a floating chimney with a height of 3000–4500 m [92] while withstanding variable external winds using its flexible accordion-like base [93]. A recently published study proposed a novel wavy ground absorber design illustrated in Fig. 15. Mandal et al. [94] analyzed the wavy design SCPP using a 3D thermofluidic flow dynamics model, showing that a wavy absorber can enhance the output power compared with the conventional flat design. Increasing the height or amplitude of the triangular structures decrease the mass flow rate and leads to lower component efficiencies for the chimney and collector, but it leads to higher velocity and temperature of the air, thereby increasing the overall efficiency and power output. As shown in Fig. 15, the optimum design is the single triangular absorber design with the highest amplitude, which enhanced the power output by up to 59 %, and the overall efficiency is improved by 62 %. Table 4 provides the details of other works focused on geometrical parameter augmentation in SCPPs.

The studies summarized in Table 4 reveal several consistent trends across literature. Most investigations confirm that key geometrical parameters—particularly chimney height, collector dimensions, and inlet configuration—play a dominant role in determining air flow velocity, pressure difference, and power output in SCPP systems. These conclusions are widely supported by both experimental and numerical studies, which emphasize that optimal design of these parameters is essential for improving system efficiency and overall performance.

4.2. Turbine modifications

The overall efficiency of SCPPs is a function of pressure drops. Haff [16] investigated pressure drops due to friction and losses in the turbine section within 24 hours in the Manzanares prototype. It was revealed

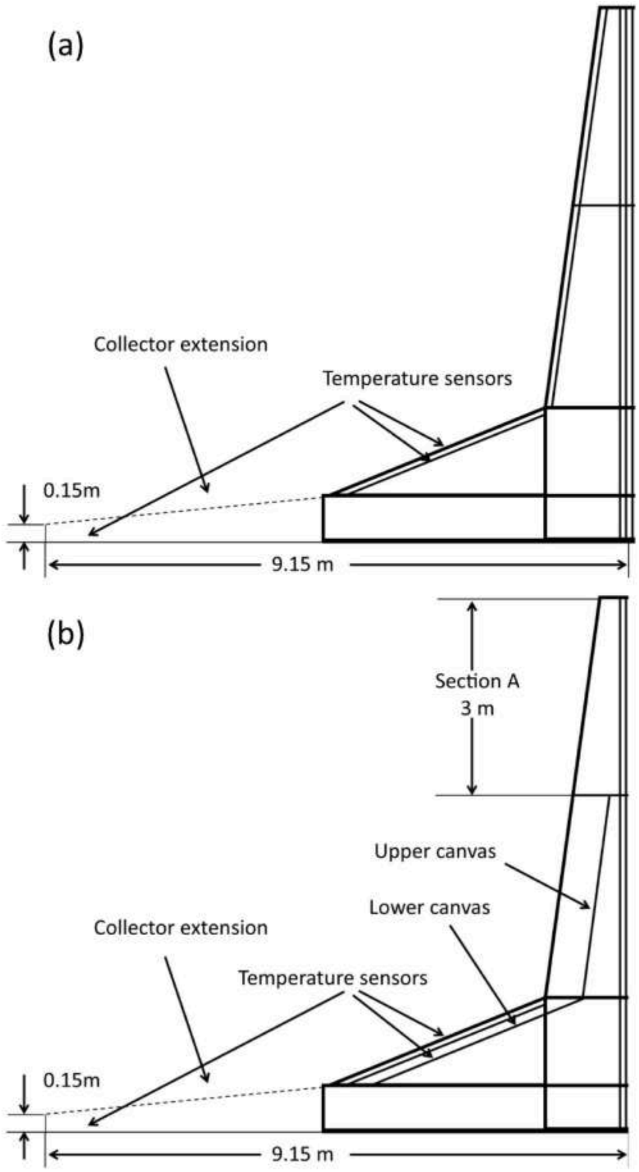

Fig. 8. Schematic of type II (a) and type III (b) solar chimneys used in the experiments (adapted from [73]).

that about 70–80 % of the total pressure drop within the Manzanares prototype occurred in the turbine. Von Backstrom and Fluri [70] analytically investigated the optimum ratio of turbine pressure drop to the total pressure drop, to produce maximum power output. They concluded that the optimum pressure ratio value was a function of air mass flow rate to the power of the negative sign of the collector floor-to-exit efficiency. Fluri and von Backstrom [95] studied the performance of single-rotor and counter-rotating turbines with and without guided vanes using an analytical model. Their model predicted very low efficiency for single-rotor turbines without guide vanes. The counter-rotating turbines showed higher efficiency at relatively low speeds. Tingzhen et al. [96] performed 3D numerical simulations of a solar tower using turbines with 3 and 5 blades. Results predicted that the 3-blade turbine produced 50 kW of power output while the larger megawatt-scale 5-blade turbine could produce 10 MW of power with an efficiency of 50 %. The effect of using three different turbine configurations of a single vertical axis, multiple vertical axes, and multiple horizontal axes on solar tower efficiency has also been investigated [43]. It was found that the single vertical-axis turbine gave higher efficiency at the cost of huge output torque, which would introduce other challenges to power generation. Nizetic and Klarin [97] analytically investigated the effect of turbine pressure drop on the power output of an SCPP. The ratio between the turbine pressure drop and the total pressure drop was found to be in the range of 0.8–0.9 to get maximum power output for different air mass flow rates. The pressure drops around the turbine, the airflow rate through the turbine, and the rotational speed of the turbine are the three important factors defining the performance of an SCPP. In this regard, Esmail et al. [98] numerically evaluated three different turbine blade designs, which are based on the so-called matrix through flow method (MTFM), the classic blade element theory (BET), and a modification of the BET-based design. It was concluded that the modified BET design outperforms the two other designs due to higher rotational speed, while the classical BET design achieved the highest mass flow rate through the turbine. Elsayed et al. [99] integrated vortex bladeless wind turbines (VBWT) inside the chimney and explored their performances through experimental and numerical studies. This research provides a comparative analysis between a conventional solar chimney with a horizontal axis wind turbine, a new configuration with a vortex bladeless vibrating rod energy harvester with four units of piezoelectric discs attached to it, and a combined configuration from the two previous designs (Fig. 16). In the VBWT concept, the vibration caused by external airflow is converted into electrical power via the piezoelectric effect. Results demonstrated an increase in power generation with the VBWT system in tandem with a turbine, which could make future SCPP development more attractive to investors.

4.3. Collector material modifications

In 2006, Pretorius and Kroger [42] evaluated the performance of a large-scale solar chimney power plant. They studied the effect of a recently developed convective heat transfer equation, collector roof glass quality, different soil types underneath the collector, and a more reliable turbine inlet loss coefficient on the power plant's efficiency. Their findings showed that by employing the new heat transfer equation, the output power decreased by 11.7 %. Using better quality glass exhibited a 3.4 % rise, while modifying the turbine coefficient led to a 0.6 % rise in annual power plant generation. On the other hand, the effect of using Limestone and Sandstone soil is the same as the original model using Granite. In another study, Elsayed et al. [99] explored different absorber materials and proposed shredded rubber as an efficient candidate for heat absorption in solar chimney collectors, which could be an eco-friendly solution for hybrid systems.

4.4. Hybrid solar designs

Although an SCPP can be operated as a standalone energy unit, sometimes other types of solar systems are employed in the solar chimney facilities to increase the total efficiency per absorbed solar energy. This section addresses several possible solar combinations to highlight the flexibility of SCPPs in combination with other solar technologies.

4.4.1. PV combination

The idea of integrating solar photovoltaic (PV) panels into a solar chimney power plant was investigated by Ahmed and Hussein [100] to introduce a co-generative system that uses both solar photovoltaic and thermal power for electricity generation. The two alternative designs that were studied in this work include a solar chimney with PV panels installed under the collector glass cover, acting as the absorber (Fig. 17a), and one with PV panels as the collector roof cover and plywood as the absorber of the chimney (Fig. 17b). Conducting the experiments in a small-scale prototype showed that employing the glass cover above the PV panels could increase the heat gain on the system, which, on one hand, increases the conversion of thermal power to kinetics and on the other hand decreases the PV efficiency due to the temperature rise on the cells. Therefore, the total useful power

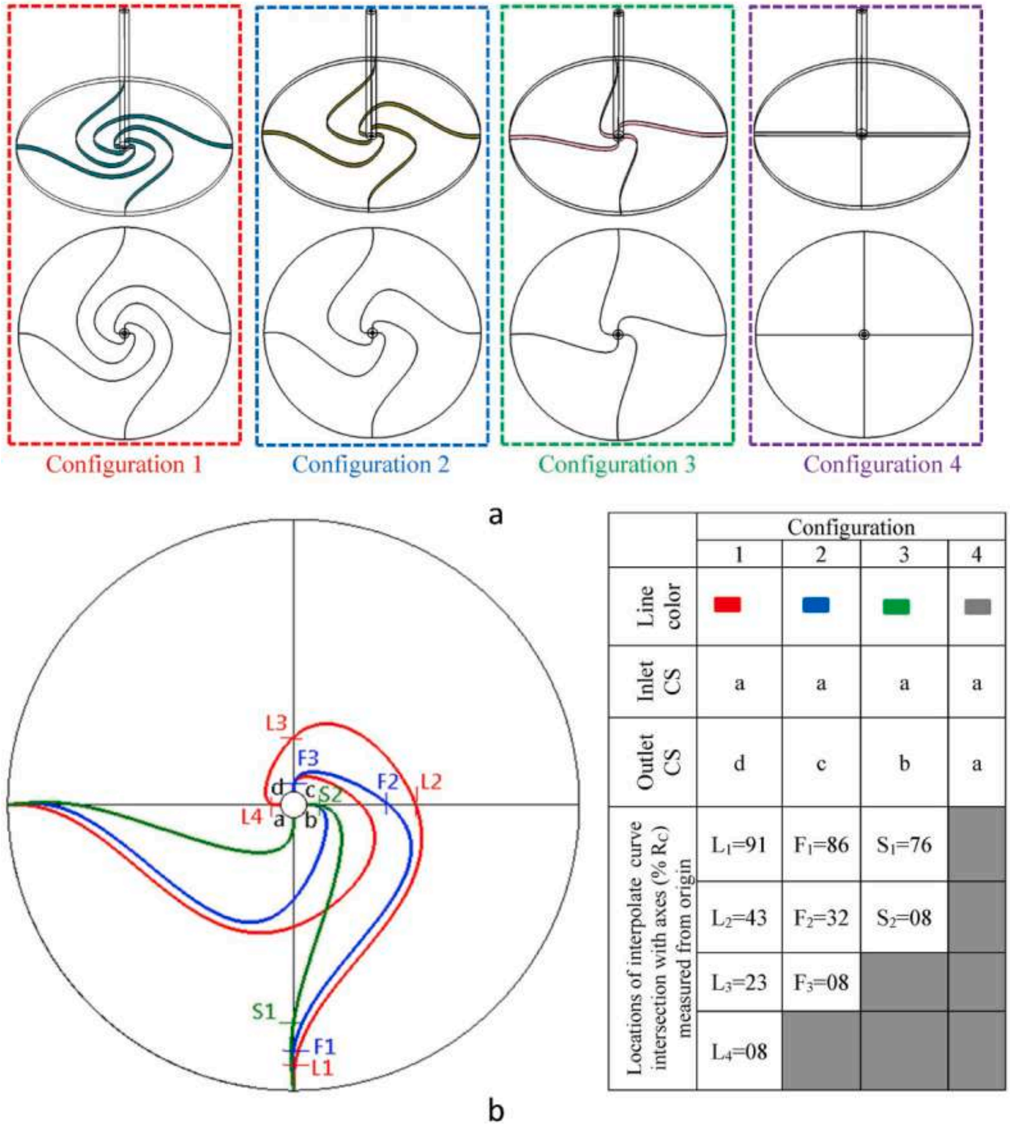

Fig. 9. Modified SCPP swirl guide blades (a) 3D CAD view of the proposed configurations (b) layouts of the interpolations used in each design (adapted from [77]).

Fig. 10. Experimental set-up of the model-scale solar chimney [78].

production would be more significant when the PV panels are used as the roof cover. In another study [101], scientists attempted to ease the

Table 3
Effect of collector inlet size on the model-scale solar chimney's output power [78].

Collector inlet height (cm)	Chimney diameter (m)	Max. air temperature (°C)	Max. air velocity (m/s)	Output power (W)*10^{-3}
6	0.2	61.8	1.3	21.97
8	0.2	48.4	1.19	16.85
12	0.2	48.2	1.04	11.24

temperature rise on the PV surface by adding a cooling system to the PV systems integrated with the SCPP. The proposed solar chimney PV/T power plant enhanced the PV efficiency by up to 4.72 %, and the lowest temperature rise and wind velocity were attained at a solar collector ratio of 0.4 and 0.6. Jamali et al. [102] explored a novel design for SCPPs, using semi-transparent PV panels as the collector roof of a solar chimney to promote the panels' cooling. As shown in Fig. 18a, applying semi-transparent PV panels allowed a fraction of the solar radiation to pass through the uncovered area, reaching the ground under the collector. Thus, the produced buoyancy force and the chimney effect drive an airflow under the PV panels, which cools the panels and increases PV efficiency (Fig. 18b). The employment of mathematical models and

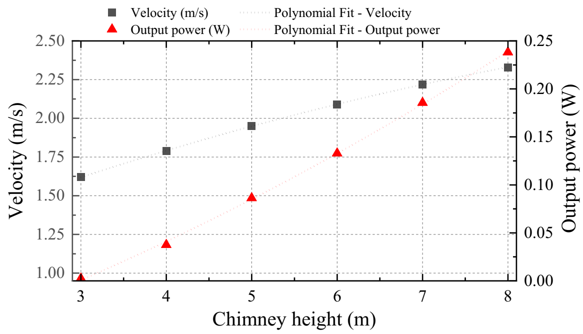

Fig. 11. Effect of the chimney height on the performance of a solar updraft tower [82].

verifications with experimental results revealed that when the semi-transparent PV system is combined with an SCPP, energy production is enhanced by 11 % compared to the conventional PV plants, used in locations with high solar flux.

These findings are consistent with later investigations of hybrid solar chimney systems, where photovoltaic modules are integrated with the collector to simultaneously generate electricity and enhance air heating, thereby improving the overall energy utilization of the system [31,103].

4.4.2. Concatenated solar systems

One of the ways to intensify the thermal driver in SCPPs is to increase solar radiation through flat reflectors or solar concentrators. In this regard, Shahreza and Imani [104] conducted an experimental and numerical study on a small-scale solar chimney to evaluate the effects of increasing solar intensity on the chimney's performance. Applying the RNG $\kappa-\varepsilon$ model with the SIMPLE algorithm, CFD simulations showed that the presented design could increase the air velocity inside the chimney, resulting in higher power production. Ouédraogo et al. [105] used several mini hemispherical concentrators in the collector area of a small-scale prototype to investigate the enhancing effects of the concentrator on the temperature and velocity profiles of air. The advantage of inserted concentrators was the ability to concentrate the incoming solar radiation independent of the time and the incident angle. The experimental results indicated that this modification reduced the heat backflow near the inlet section, while the thermal and dynamic fields improved by 24.4 and 58.6 %, respectively. In another attempt, Khidhir and Atrooshi [106] redesigned an SCPP using a tracking mirror reflector. The studied small-scale power plant was built with a circular collector segment, equivalent to one-third of a circle of 9 m diameter, having an inlet height of 0.3 m, which was increased to 1.35 m near the chimney inlet. The chimney was a 6 m cylindrical column located in the center of the collector, creating a maximum height of 7.35 m from the ground. The reflector was a flat mirror with a height of 1.5 m and a width of 1 m, placed to the north of the system, with an 11 m distance from the periphery of the solar collector. Furthermore, an extended absorber area was mounted vertically at the base of the chimney to absorb the reflected solar radiation, as shown in Fig. 19. Therefore, the concentration effect in the transition zone, where the air enters the chimney after the collector, was responsible for a further increase in air temperature, intensifying the buoyant force that directly affects the dynamics of airflow in the solar chimney. A 10.25 % growth in the maximum temperature at the inlet of the chimney and a 22.22 % enhancement in the maximum airflow velocity were observed.

Hussain and Al-Sulaiman [107] analyzed an SCPP performance enhanced by solar reflectors using experimental and numerical studies. After validating the numerical results with the experimental results, it was found that adding solar concentrators increased the ground temperature and air mass rate by 9.89 % and 134 %, respectively, compared with the conventional designs. Also, energy efficiency and power output were enhanced by 22.61 and 133 %, respectively.

4.4.3. Solar pond

In principle, solar ponds are a type of low-temperature power generation system among solar technologies. During the operation, solar ponds turn into solar collectors by forming different thermal layers, depending on the salinity of the water. Since the salinity gradient surpasses the natural convection, the absorbed solar radiation at the bottom of the pond accumulates in the lowest layer (with the highest brine concentration), increasing the water temperature. Akbarzadeh et al. [108] performed a feasibility study on the various combinations of a solar pond with an SCPP. Two alternative configurations were suggested in that study, as shown in Fig. 20. In the first design, hot brine was extracted from the bottom layers of the pond and then injected (through a water-to-air heat exchanger) into the chimney to the incoming air and drive a further temperature rise in the chimney. However, in the second design, the heat was exploited with a non-direct contact heat exchanger to work on the same principle. They asserted that although the proposed designs are viable to produce power in an efficient way, the problems with such hybridizations are the higher pressure drop through the heat exchanger, the pumping power, cost, and corrosion.

In another study, Zhou et al. [109] aimed to use a solar pond for the night operation of an SCPP through mathematical modeling. Results showed that if an SCPP that produces 5 MW of power during daily operations is coupled with a solar pond of the proper size, then the nocturnal power production is as high as 2.21 MW.

4.5. Integration with thermal energy storage

The ground under the collector is a natural thermal energy storage as it stores the thermal energy achieved from solar radiation during the day and releases it when the ambient temperature decreases (e.g., during the night). This behavior significantly affects the SCPP performance and operating time [110], and helps to have a daily continuous power generation [111]. Therefore, several studies proposed and evaluated different alternative materials to cover the ground to achieve more effective heat storage. The soil is a natural heat storage whose thermal inertia increases as its compaction degree increases, leading to a better thermal storage medium. Hurtado et al. [111] studied the effect of soil thermal properties under the collector on the performance of an SCPP numerically. The transient numerical model showed a 10 % increase in the power capacity of the SCPP by increasing the soil compaction degree. Ming et al. [112] proposed a storage system of water and sandstone integrated with an SCPP to minimize the fluctuations in output power. The mathematical model showed that the hybrid system produced smoother power output with an optimal depth of water storage system in the range of 5–20 cm. Ikhlef et al. [113] experimentally evaluated the effects of different materials as thermal storage placed in the collector base such as soil, sand, water, PVC tube, and gravel. The results showed that the crushed gravel, which has higher thermal conductivity than the other materials, was the best option for storing heat, where the collector efficiency improved, reaching 89.7 %. Another experimental work performed by Chaichan and Kazem [114] also confirmed that using pebbles (gravel) as a collector base improved the SCPP efficiency. However, these experimental measurements were for small SCPP prototypes and may not be precisely reliable for large-scale plants. While the mentioned materials act as sensible heat storage, some phase change materials, such as paraffin, have also been proposed as latent heat storage. For example, Fadaei et al. [110] applied a paraffin wax-filled and sealed layer of 1 cm thickness as an absorber placed on the ground under the collector of a prototype SCPP. The used paraffin wax has a solid phase at room temperature, and begins to melt at around 45 °C. Their experimental results showed an enhancement in the performance of the system.

Although different storage materials and configurations have been investigated, the literature consistently reports that integrating thermal energy storage improves the stability and duration of SCPP operation by maintaining the temperature difference driving the airflow after sunset [35,115].

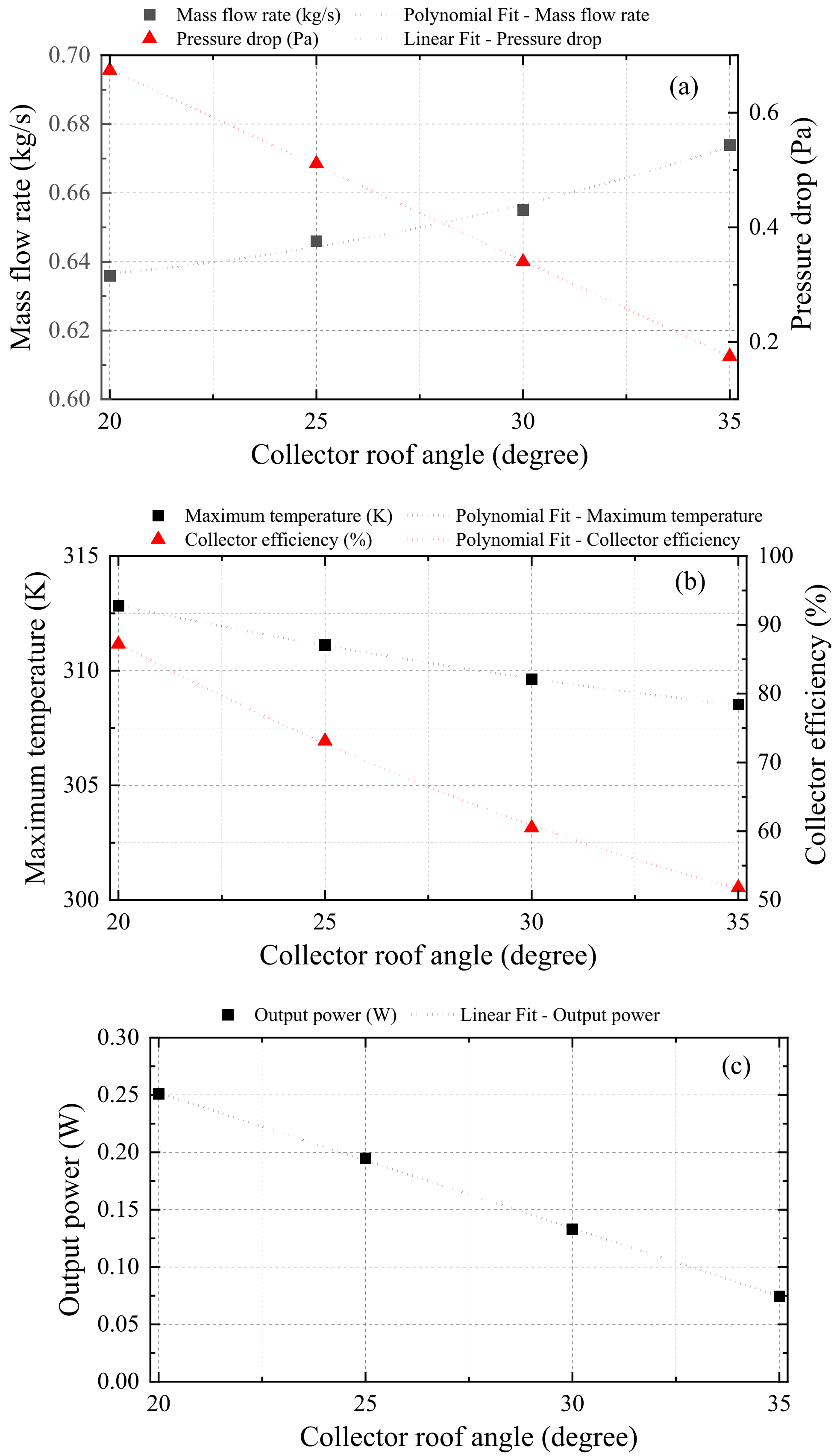

Fig. 12. Effect of the collector roof angle on the performance of a solar chimney tower [82].

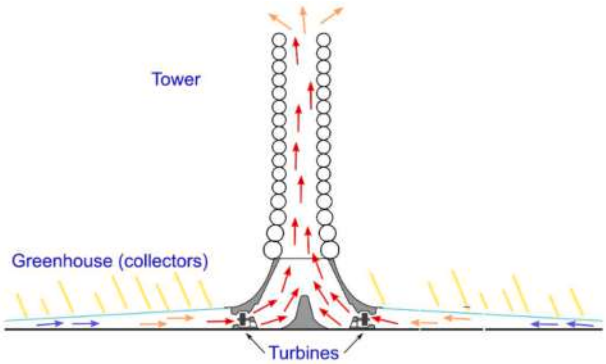

Fig. 13. Schematic of an inflatable chimney consisting of a free-standing stack of hollow gas-filled tori [88].

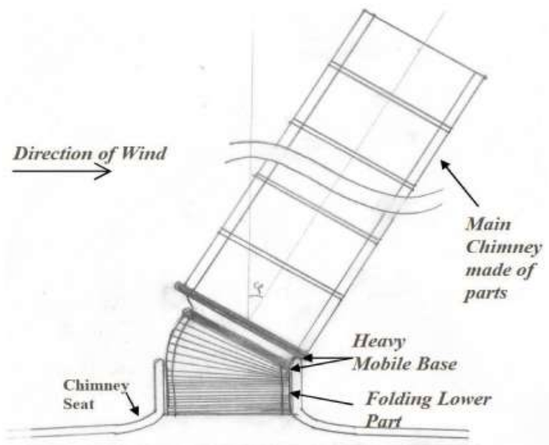

Fig. 14. Schematic of the floating solar chimney made of a reinforced fabric core and a set of BOPET/HDPE lifting tubes filled with lighter-than-air gas [91].

4.6. Integration with desalination units

A poly-generation concept has been formed out of the combination of solar chimneys and desalination systems, leading to the simultaneous production of electricity and fresh water from renewable energy sources. Moreover, integration of poly-generation into SCPPs could improve economic feasibility [116]. In this way, Zuo et al. [117] incorporated a basin solar still below the solar collector, as well as a rock energy layer as the absorber (see Fig. 21). Thus, the absorbed solar energy was transmitted to the still, where the water body reaches the highest temperature. As the seawater was heated during the operation, the produced water vapor was later condensed on the inner side of the glass cover to be collected as freshwater. For more detailed performances, Zuo et al. [118] developed a small-scale SCPP prototype integrated with a solar still and observed that the maximum water production occurs when solar irradiance is absent. Moreover, the outermost 1/3 section of the collector radius has the highest contribution to the air temperature rise. One of the shortcomings raised in these hybrid SCPPs is that the temperature and velocity of the airflow inside the chimney are lower than those of the conventional SCPP models due to the release of vapor latent heat as the air rises up the chimney [119]. In this regard, Azad et al. [116] used a machine learning technique to optimize the balance between power generation and freshwater production in a dual-purpose SCPP. Using a 2D CFD analysis, the optimized geometric design led to the power and freshwater production of 719 kW and 14.28 kg/s, respectively. Furthermore, it was seen that the growth of the collector diameter increased the evaporation rate, while a rise in chimney height could improve the vapor condensation due to higher air temperature reduction. In another numerical study conducted by Zuo et al. [120], the effects of turbine designs, including different blade numbers, installation angles, and relative radial clearances, on freshwater productivity were investigated. The obtained results indicated that the presence of a guide cone and guide vane has a positive effect on the flow field, and increasing the radial clearance of turbine blades would improve the system's freshwater productivity.

Abdelsalam et al. [121] proposed a novel sustainable water and electricity generation approach by combining an SCPP with a cooling tower and a solar basin. In this concept, a bidirectional turbine is integrated with a conventional cooling tower, which provides the base structural foundation. The SCPP operates during the daytime, utilizing

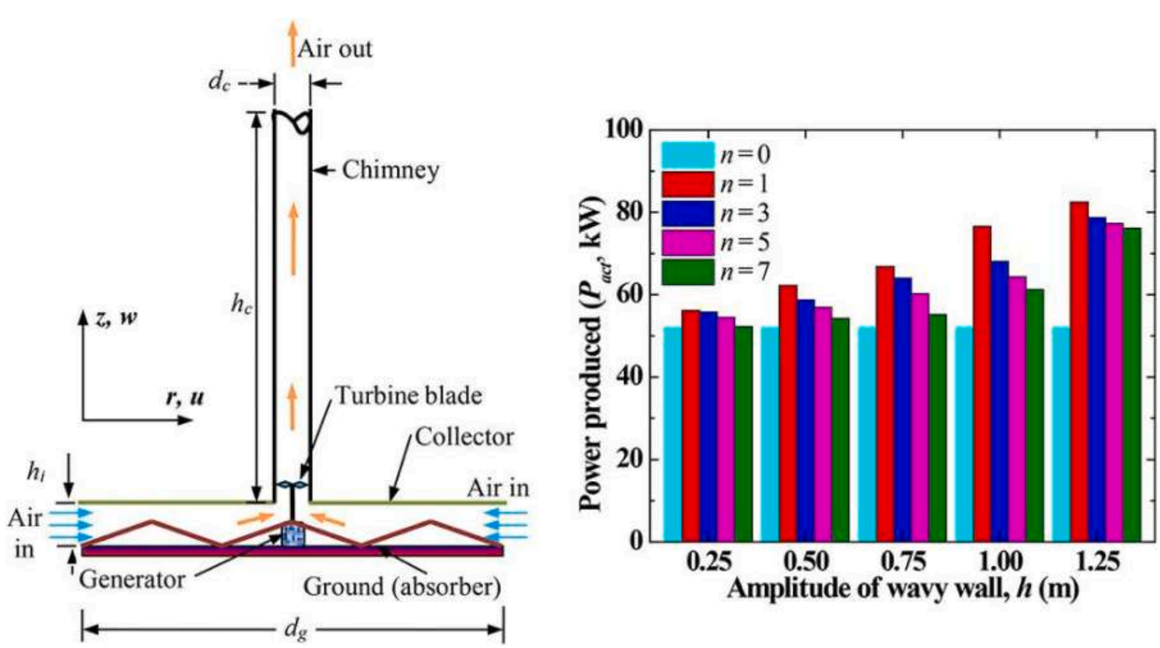

Fig. 15. A wavy design of the ground absorber and the produced power [94].

Table 4
Selected studies focused on geometrical parameters to enhance the performance of SCPPs.

Authors	Type of Study	Scale classification/ Dimensions	Investigated parameter	Main findings
Al-Kayiem et al. [183]	Experimental	Small-scale (H_t = 6.5 m, R_c = 3.5 m)	Effects of condensate film formation	Condensate film reduces solar transmissivity (~10 %), delays collector heating (2–3 h evaporation), and lowers air temperature rise by 3–5 °C, suggesting the need for auxiliary heating before sunrise.
Mehdipour et al. [184]	Experimental	Small-scale (H_t = 1.94 m, R_c = 1.13 m)	Collector geometry (altering the shape from circular to square)	Square collector geometry avoids airflow restrictions near the chimney, improving Nusselt number (1225 %) and thermal efficiency (169 %) compared with circular collectors.
Sheikhnejad et al. [185]	Numerical	Small-scale	Passive vortex generator inside the solar chimney	Passive vortex generators increase temperature and thermal efficiency despite slight airflow reduction, with stronger effects at high solar flux.
Toghraie et al. [186]	Numerical	Medium-scale (H_t = 100 m, R_c = 4 m)	Geometric parameters	Larger chimney height and collector radius improve power output, while higher collector height reduces performance.
Cao et al. [187]	Numerical	Large-scale (H_t = 700 m, R_c = 550 m)	Double-chimney power plant and tilted and horizontal solar collectors.	Double-chimney configuration reduces required chimney height while significantly increasing annual power output compared with conventional SCPP systems.
Aziz and Elsayed [188]	Numerical	(H_t = 20- 30 $R_{turbine}$, R_c = 35 - 55 $R_{turbine}$)	Geometric parameters	Optimal chimney angle (~3°) and inlet height improve airflow velocity and thermal efficiency, while a concave chimney reduces flow separation and energy losses.
Cuce et al. [189]	Numerical	Manzanares-scale (H_t = 194.6 m, R_c = 122 m)	Ground slope	Moderate ground slopes (~0.5°) increase the turbine pressure difference and improve power output, while larger slopes (>1°) reduce performance.
Nasraoui et al. [190]	Experimental and numerical	Manzanares-scale (H_t = 194.6 m, R_c = 122 m)	Double-pass counter flow solar collector	Double-pass collector increases fluid temperature and velocity and improves collector efficiency (~28 %).
Abdelsalam et al. [191]	Numerical	Medium-scale (H_t = 200 m, R_c = 125 m)	Double-chimney (co-centric secondary external chimney)	Double-chimney design enables day and night power generations using the inner and outer chimneys, respectively, reducing the levelized cost of energy (LCOE) by ~50 %.
Singh and Kumar [192]	Numerical	Small-scale (H_t = 3 m, R_c = 1.5 m)	Chimney guide vane	Guide vane with an optimal chimney divergence angle (~2°) enhances updraft and increases theoretical power output by more than 770 %.
Xiong et al. [193]	Numerical	Medium-scale (H_t = 200 m, R_c = 60 m)	Wind-resistant structures	Partition and porous walls mitigate crosswind effects and stabilize

(continued on next page)

Table 4 (*continued*)

Authors	Type of Study	Scale classification/ Dimensions	Investigated parameter	Main findings
				power generation.
Mandal et al. [194]	Numerical	Manzanares-scale (H_t = 194.6 m, R_c = 122 m)	Chimney geometry (sudden contraction and expansion)	Sudden expansion and sloped absorbers improve performance, while contraction has little effect.
Mandal et al. [195]	Numerical	Manzanares-scale (H_t = 194.6 m, R_c = 122 m)	Geometric parameters	Thermo-economic optimization of chimney and collector dimensions significantly improves SCPP power output (up to 3.82 ×) and efficiency (up to 4 ×) at comparable cost to the Manzanares plant.

the heated air's lower density to promote mechanical work and produce electricity and freshwater. During the nighttime, the chimney functions as a cooling tower, using a water mist sprayer to evaporate water at the top of the chimney and cool the dry air, which then gets denser and moves downward through the turbine, generating electricity before exiting the tower. Fig. 22 indicates the dual functionality of the proposed hybrid design for sustainable water and electricity generation. In a recent study, Abdelsalam et al. [122] introduced a hybrid solar double-chimney power plant (HSDCPP) to enhance energy output density per unit of construction area. This system operates as a cooling tower at night and functions as both a solar chimney and a cooling tower during the day. Results indicated that the HSDCPP's annual energy production was 3.83 times higher than that of a traditional solar chimney of similar dimensions. Additionally, unlike the traditional solar chimney, the HSDCPP produces fresh water as well as renewable energy.

Zuo et al. [123] conducted an experiment to explore the operational parameters of an SCPP integrated with a distillation system. In this design, six individual solar stills were formed under the heat collector in a radial and modular design. The obtained results indicated that the daily water yield per unit area of the solar still decreases radially the closer the still is to the chimney, and the peak period of water productivity is achieved between sunset and 1–3 am. Moreover, a constant temperature increase of 5 °C was observed for operations during the night. Mendez and Bicer [124] investigated the possibility of using an SCPP and a wind turbine to empower a hybrid desalination system composed of reverse osmosis (RO) and a multi-stage flash (MSF) system. In this concept, a heat storage system was also integrated with the SCPP to store the excessive heat from the collector area and provide thermal power for the MSF system. The brine rejected from the first desalination unit is further treated in a membrane-based RO unit to increase water productivity, while the SCPP and wind turbines produce the electricity required to operate the RO system. The numerical analyses conducted in Engineering Equation Solver (EES) revealed that the combined configuration could increase the SCPP energy efficiency from 0.5 % to 50 %, producing 8.3 kg/s of fresh water as well. It should be noted that the efficiency figure arrived at by Mendez and Bicer includes additional energy-generating facilities (multiple MW-scale wind turbines) and the desalination products in their efficiency calculations and does not reflect a 100-fold improvement on the thermodynamic efficiency of the SCPP itself. Alkasrawi et al. [103] proved that adding PV panels to the collector circumference of an SCPP can improve the performance of a combined SCPP and desalination system. The reason refers to the synergy effect that comes from the cooling of PV panels and preheating the feeding air that takes place underneath the PV modules. Therefore, the results showed that annual electricity production increased from 380 to 494 MWh, while water production increased from 278 to 326 thousand tons/year. The numerical study by Tawalbeh et al. [125] showed that adding PV to the combined SCPP and desalination system increased the efficiency to 52.1 %. As with the calculations performed by Mendez and Bicer [124], these figures rely on additional electrical generation sources and do not represent a direct improvement in the thermodynamic efficiency of the SCPP itself. Additionally, the effect of geometrical parameters was analyzed, revealing that increasing the chimney height and collector radius enhanced efficiency, while increasing the collector height reduced efficiency. Regarding economic matters, Abdelsalam [126] showed that an integrated SCPP-desalination system could provide annual electricity and water production of 81,440 kWh and 123,753 tons simultaneously, reducing the LCOE of SCPP to 1.86 $/kWh.

Abedi et al. [127] investigated the feasibility of combining a humidification–dehumidification system with a solar chimney power plant to create a solar desalination chimney (Fig. 23). This innovative system utilized solar energy to produce buoyant hot air that flowed

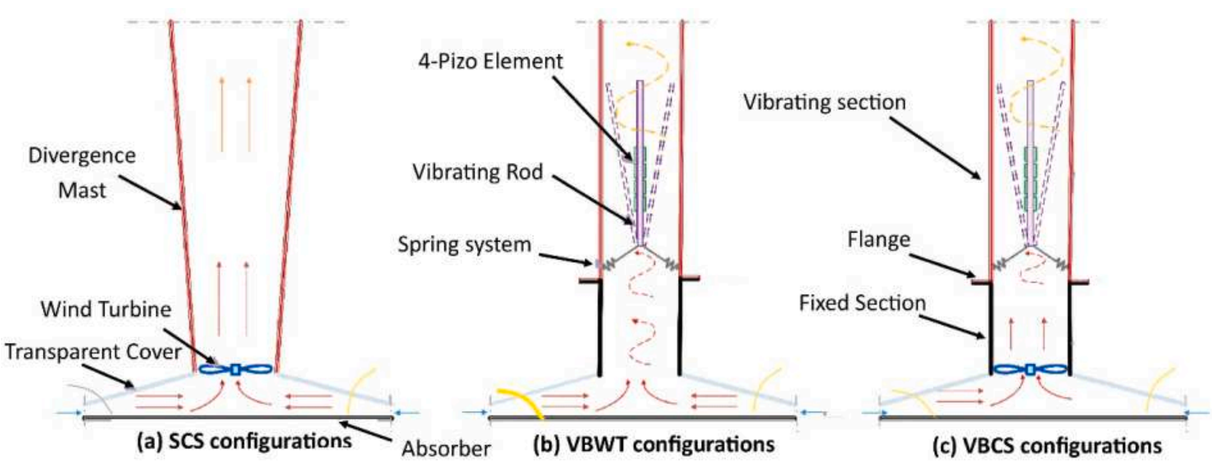

Fig. 16. Schematic illustration of various energy harvesting configurations using a solar chimney (adopted from [99]).

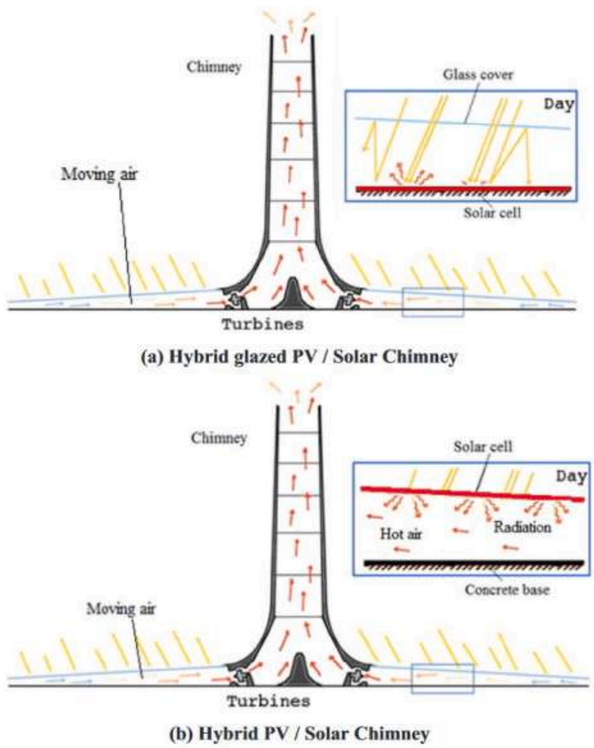

Fig. 17. The concepts of the PV integration with the solar chimney, as proposed in Ref. [100]; (a) PV is integrated as the collector absorber, (b) PV is integrated as the collector roof.

through the humidification–dehumidification process. A turbine was integrated to generate power for circulating water, contingent on adequate airflow. In the modified Manzanares chimney, the diameter was expanded to three times its original size, which decreased pressure loss and increased airflow mass, enabling the system to provide fresh water to over 800 households (600 tons/day). The study also found that this SCPP configuration could be scaled down to fit on a rooftop and satisfy daily water needs for individual residences. Zuo et al. [128] provided a corrugated plate configuration for the solar absorber section of the still unit through an experimental endeavor. As a result, the increased surface area enhances solar absorption, leading to a rise in the heat transfer rate and reducing the time required to preheat seawater. This accelerates the evaporation of seawater in the still and boosts power generation and freshwater production by 5.24 and 17.87 %, respectively. Abdelsalam et al. [129] conducted a numerical study to model an SCPP incorporated with a water desalination power plant in Qatar. This system aims to redirect the excessive heat from a water desalination power plant to the collector of an SCPP, and increase the electricity efficiency as well as water distillation. As a result, the new design led up to 72 % higher water production compared to the previous combined designs, bringing also 74 % more power generation.

A novel concept was established by Zou et al. [130] by introducing multilayer collector flow channel structures, focusing on the geometric characteristics of the double-layer collector. As shown in Fig. 24a, in the simple design, the distillation pool is circular and located beneath the collector, consisting of a total of 117 rings. The airflow pathway is radial, and the double-glass glazing reduces the thermal losses to the ambience. Fig. 24b presents a dual-channel parallel-flow type collector, where two parallel flows form as the air moves radially and converge in the transition section. This improves the system's performance by decreasing the thermal losses, similar to the double-glass roof design. Another configuration was made as Fig. 24c, in which a single-channel counter-flow is employed to expand the path of hot airflow in the

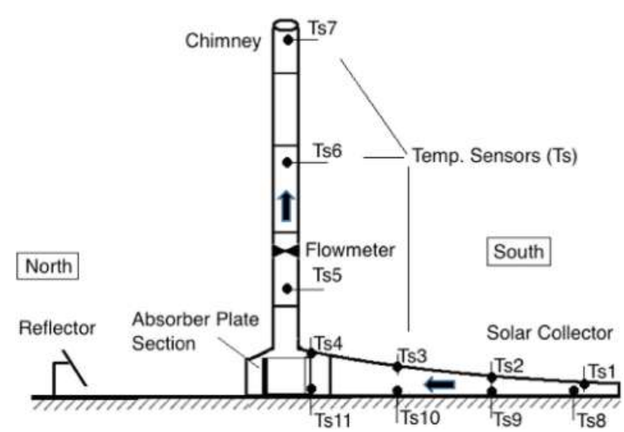

Fig. 19. The schematics of the reflector integration with an SCPP [106].

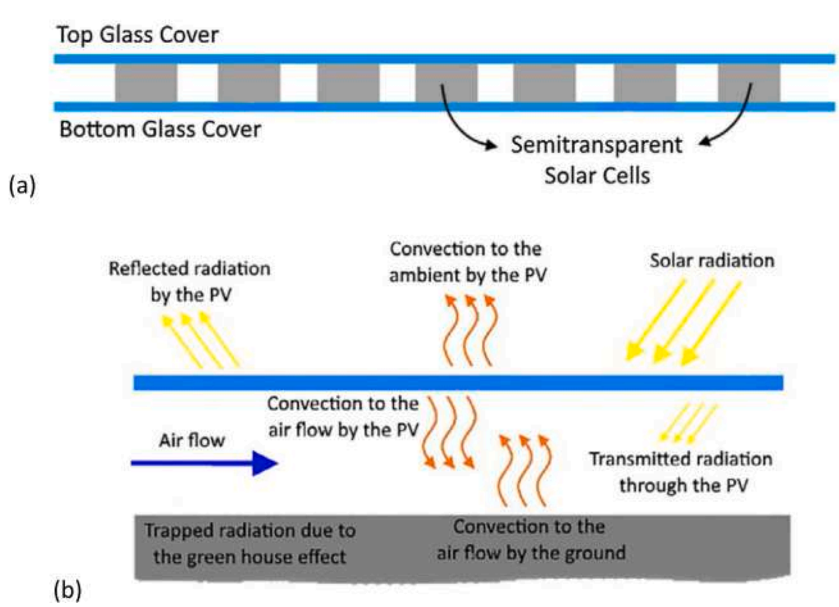

Fig. 18. (a) Semi-transparent PV wafer, (b) heat transfer mechanism in a PV-SCPP (adopted from [102]).

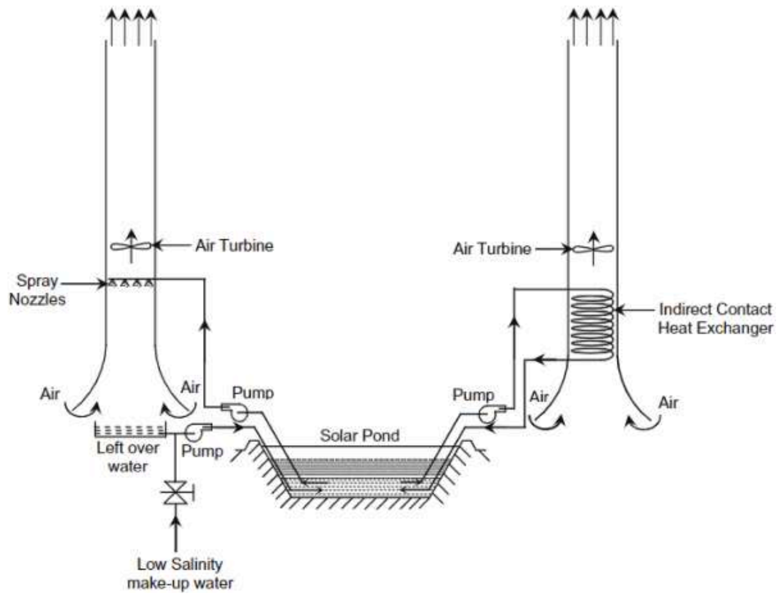

Fig. 20. Two concepts for the combination of an SCPP with a solar pond plant [108].

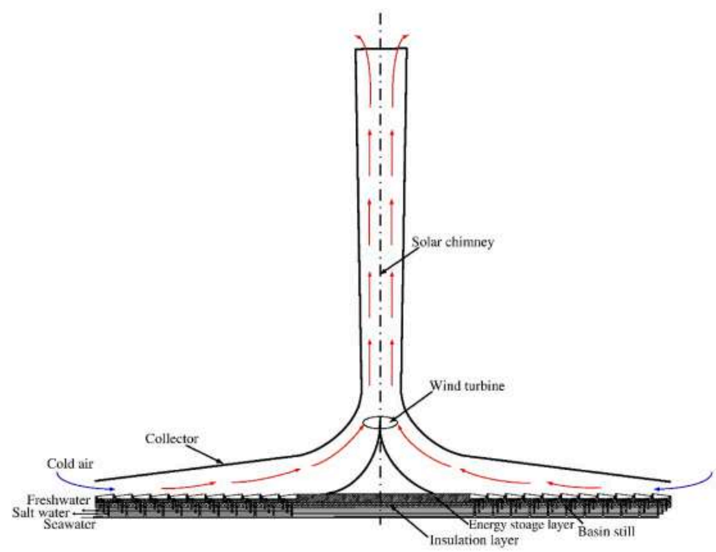

Fig. 21. Schematic of an SCPP coupled with a solar basin still [117].

collector and improve the contact time between the collector and air, leading to higher heat transfer and an increased energy gain. In the second passage, the air moves above the distillation pool cover towards the base of the chimney, which absorbs the heat from the pool cover. However, in the next configuration (Fig. 24d), air moves below the distillation pool, and the second heat transfer occurs between the air and the absorber of the distillation pool, which undergoes a higher temperature than the previous design. Numerical simulations revealed that although all four designs improve the power output compared to the conventional SCPP, water production is enhanced only considering the single-channel counter-flow and surround-flow types. Moreover, the highest performance was achieved by the surround-flow type, which provides heat storage at the bottom of the collector. As a result, the average power generation for this design was 43.3 kW, which is 132.8 % more than that of the standard type.

It should be noted that the integration of desalination plants complicates the economic analysis of the SCPP in comparison to other renewable energy sources.

4.7. Integration with buildings

One of the interesting hybrid designs in emerging SCPP designs is the deployment of such power plants in urban areas and their combination with buildings. Mebarki et al. [131] conducted a CFD analysis to find a solution for the minimization of large power plants, enabling them to be incorporated in urban areas. Using the RNG $\kappa-\varepsilon$ turbulence model and discrete ordinates non-grey radiation model, they found that as the scale factor decreases, air velocity, pressure difference, and mass flow rate decrease and the temperature rises logarithmically. Moreover, if the Manzanares SCPP is rescaled by 0.76, 0.636, and 0.51 ratios, the daily energy outputs would be 191.93, 106.55, and 51.12 kWh/day, respectively. Also, Saad et al. [132] proposed a novel design where an SCPP was employed within a high-rise building for sustainable development in cities, as shown in Fig. 25. Using CFD analysis, they studied the effects of the reduction in collector angle (the angle around the chimney, which is occupied by the collector, where 360° would be a full circular collector) on the performance and operating parameters. Results indicated

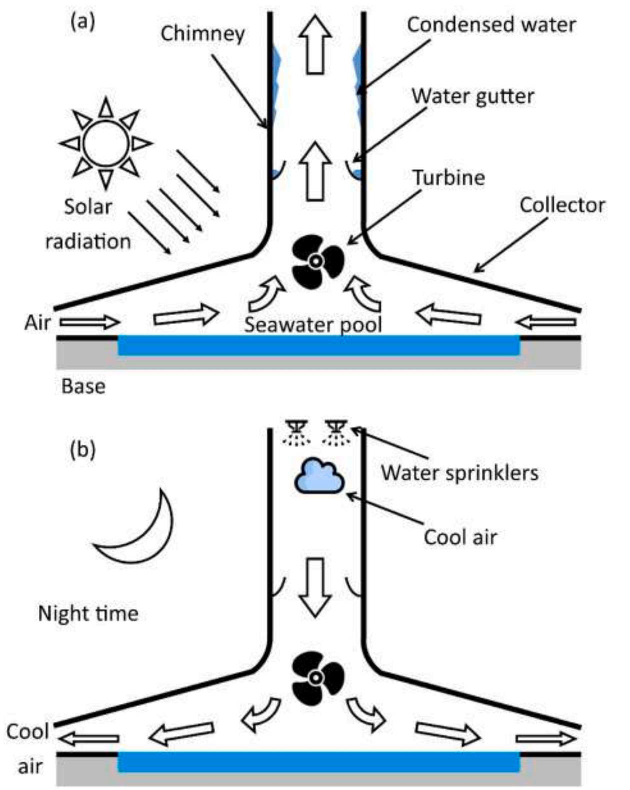

Fig. 22. Scheme of the (a) diurnal and (b) nocturnal functions of a combined SCPP and desalination system (adapted from [121]).

that a 120° or higher collector angle must be respected to achieve an acceptable power output. Moreover, when the solar angle decreased from 360 ° to 120°, the power output diminished from 47.4 kW to 26.1 kW.

Titi et al. [133] investigated the integration of a solar chimney power plant into high-rise buildings, where the building height acts as the chimney and the roof functions as the solar collector. Using CFD simulations, they showed that installing turbines at both the top and bottom of a 140 m building could produce a total power output of 33.47 kW, with 26.81 kW generated at the bottom turbine and 6.62 kW at the top turbine, demonstrating the feasibility of SCPP-based energy generation in urban high-rise structures.

Fereidoni et al. [134] recently reviewed the application of solar chimneys integrated into residential and non-residential buildings for ventilation and energy saving. Their study categorized building-integrated solar chimney systems into solo and hybrid configurations, including wall-mounted, roof-top, center-based, prototype, and inclined designs. The review also highlighted the potential of hybrid configurations combining solar chimneys with systems such as photovoltaic panels, Trombe walls, earth-to-air heat exchangers, wind turbines, and phase-change materials, which can further improve ventilation performance and reduce building energy consumption.

4.8. Integration with geothermal systems

One of the strongest points in the concept of SCPPs is the utilization of the foundation on which the plant is built, which acts as natural heat storage to ease the intermittent effects of solar power on the produced energy. However, this source is limited and requires some improvement techniques for efficient integration and ensuring a continuous operation, especially during cloudy days and nighttime [135]. For this purpose, Cao et al. [136] designed a geothermal-solar chimney power plant (GSCPP), as shown in Fig. 26. In this system, a geothermal production well is exploited to provide high-temperature geothermal water, which is stored in a heat storage pond and later used in a water-to-earth heat exchanger (WEHE) placed on the ground inside the solar collector. After transferring the heat to the ground, the geothermal water is returned to the geothermal injection well. Moreover, the presence of sand as the filler among WEHE tubes allows additional thermal storage, providing an average temperature field. The simulation results demonstrated that the power generation from the combined model is higher than the sum of the single solar and single geothermal models.

Zou and He [137] proposed a hybrid system using the waste heat from a geothermal power plant to heat up the ambient air at the inlet of the collector of a solar chimney tower plant. CFD results showed an increase of up to 20 times in the net power output for a hybrid system vs pure CSPP at the expense of reduced heat dissipation capacity for the primary geothermal system. Mokrani et al. [138] developed a GSCPP

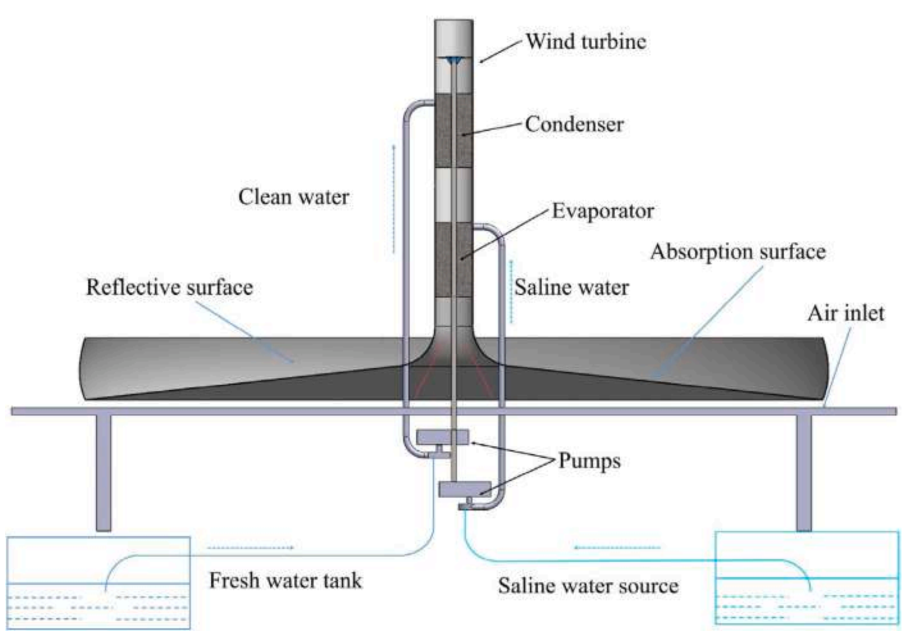

Fig. 23. A possible configuration of a water desalination process integrated with a solar chimney (adopted from [127]).

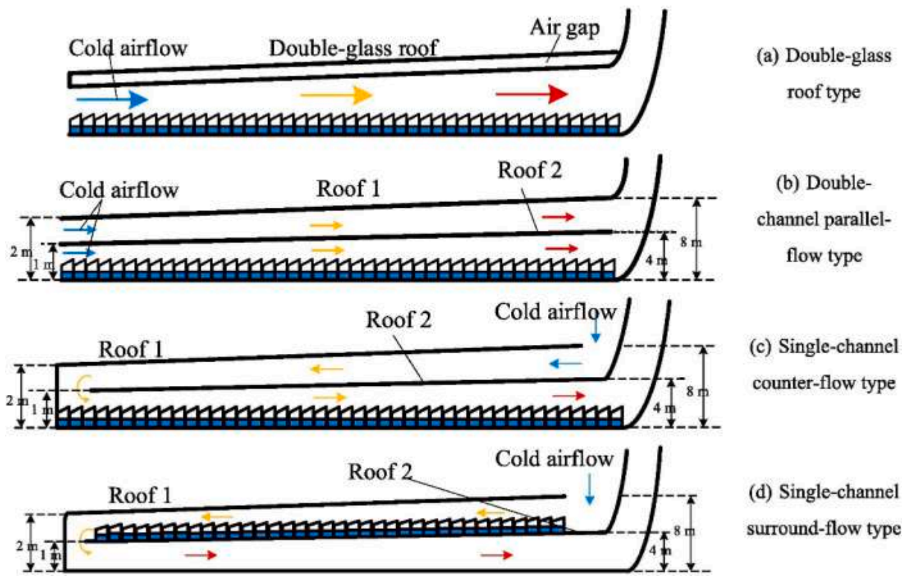

Fig. 24. Schematic design of modified collector structures in an SCPP coupled with solar desalination units (adopted from [130]).

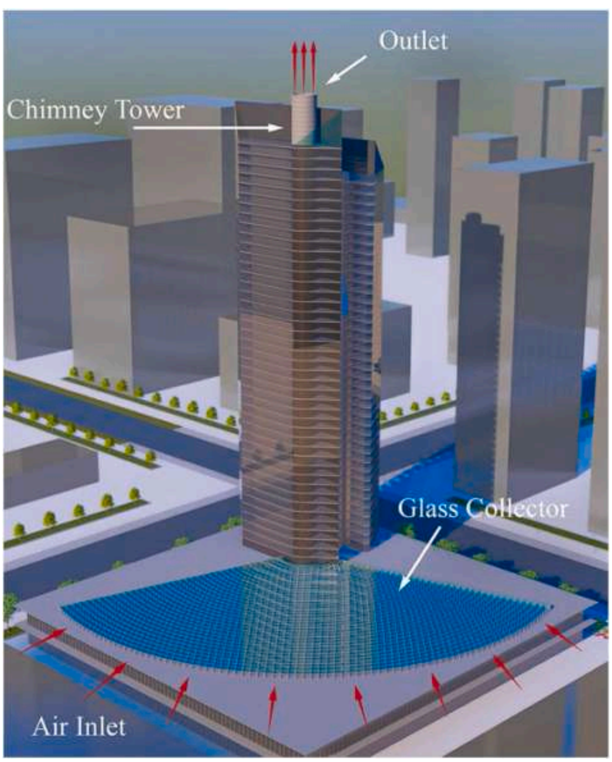

Fig. 25. The visualization of SCPP integration with a high-rise building [132].

prototype with an 8 m height and a 12 m collector diameter, using a spiral pipe heat exchanger inside the collector, as shown in Fig. 27, to use the geothermal power for the nighttime operation regardless of external weather conditions. Running the geothermal water from the center of the collector to the peripheral showed that, as the hybrid approach is used during the daytime, the collector center temperature increased from 68 °C to 80 °C, and the air velocity grew from 5.8 m/s to 7.1 m/s. Furthermore, the maximum nocturnal temperature and air velocity reached 37 °C and 5.1 m/s for the operation during the winter season. Dhahri et al. [135] located a heat exchanger made of radial tubes at the center of a classical SCPP collector to improve thermal power conditions, adding additional heat from geothermal power. Conducting a numerical study, it was found that the proposed system was able to produce more power throughout a 24-hour period.

Habibollahzade et al. [139] investigated the combination of a solar chimney with a geothermal pipe, using two trapdoors; one is closed during sunny days and lets the entire system operate as an SCPP, while when the solar radiation is mitigated or for nighttime operations, the second trapdoor is used to exploit the heat at the outlet of the geothermal pipe. For both functions, a pressure difference is made to draw in the ambient air into the collector and generate electricity through the turbine. Fig. 28 demonstrates this concept in both operating configurations. The numerical results showed that employing the proposed configuration for an SCPP at scales comparable to Manzanares would result in a continuous (24/7) power output of 3–7 kW. Moreover, properly integrating geothermal systems with SCPP decreases the LCOE of conventional systems. Further, scientists [140] introduced a multi-inlet geothermal pipe and achieved a 26 % increase in power output compared to a single-inlet pipe.

4.9. Integration with waste heat recovery

The idea of a combined/ hybrid solar cycle has been proposed in the literature to enhance the thermal efficiency of solar chimney power plants, making the final cost competitive with the electricity produced from gas and coal. In combined/hybrid cycles, waste heat from other sources/facilities is usually utilized to heat the air within the collector, enhancing the output power and efficiency of the hybrid cycle. Fathi et al. [14,141] proposed a combined solar-nuclear cycle (Fig. 29). The idea was to apply the available surplus heat from the nuclear cycle to the air within the solar chimney collector. CFD results predicted a 5 % increase in the overall efficiency of the combined cycle (See Fig. 30).

Anderson et al. [142–144] proposed to use compost waste heat within an SCPP (Fig. 31). The heat generated during the composting process is used to heat the air within the collector to increase the rising air temperature and velocity within the chimney and therefore enhance the output power. The hybrid solar/compost waste heat power plant with a 1150 ft tall chimney of 24 ft diameter processing 8000 tons of composting material showed a 34 % increase in the net output power [142]. Azeemuddin et al. [145] and Al-Kayiem et al. [146] investigated the effect of utilizing waste heat from a gas turbine power plant to heat the air within a solar chimney tower plant. The flue gas flowed within channels passing through the collector inlet up to its exit to heat the air.

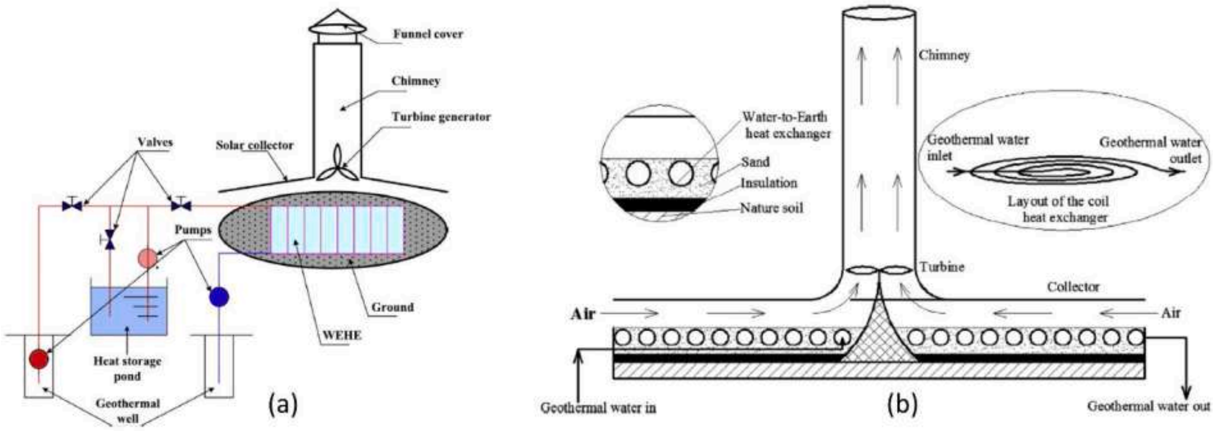

Fig. 26. The layout of a geothermal-SCPP; (a) schematic of the main components (b) design of the geothermal subsystem (adopted from [136]).

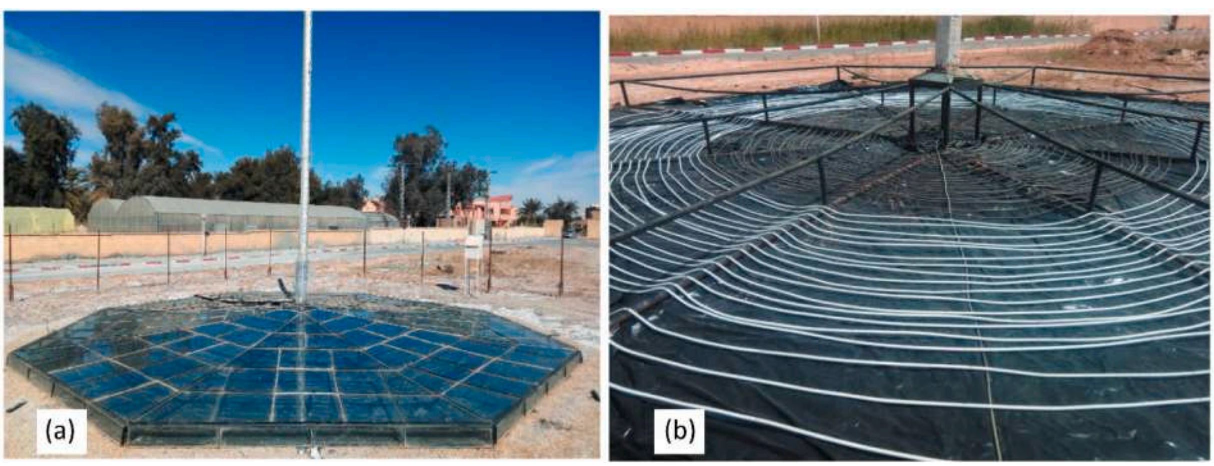

Fig. 27. Photograph of the prototype fabricated for small-scale GSCPP; (a) prototype, (b) photograph of the employed spiral heat exchanger (adopted from [138]).

The main idea was to enhance the power production rate at night when the solo SCPP output usually decreases. The combined system was shown to increase the net power output by 30 % while improving SCPP power production after sunset.

Zandian and Ashjaee [147] used the rejected heat within the condenser of a 250 MW steam power plant to heat the ambient air at the inlet of the collector of an SCPP. The hybrid system was reported to have a 30 % higher power output. Ghorbani et al. [148] proposed a conceptual design for a hybrid system using waste heat from a steam power plant to increase the air temperature entering the collector while injecting the stack of hot flue gas into the rising air in the chimney. This injected hot flue gas generates suction power and increases the airflow rate within the collector inlet. CFD results showed almost 0.54 % enhancement in the overall thermal efficiency of the steam power plant. Hu and Leung [149] studied the fluid flow within a solar waste-heat chimney power plant. The hybrid system used the waste heat from a 30 MW fossil fuel power plant to heat up the ambient air entering the collector. 3D CFD simulations using a compressible ideal gas airflow model predicted a 50 % increase in the output power of the hybrid system over a conventional solar chimney tower plant. Aurybi et al. [150] evaluated the performance of an SCPP using an external heat source from hot flue gas passing through four channels within the collector (0.002 kg/s hot gas flow at a temperature of 100 °C). The steady-state CFD analyses revealed 24 % and 56 % enhancement in air velocity within the chimney and output power, respectively. Esmaili et al. [151] investigated a novel SCPP combined with a flare gas combustion to exploit the energy lost in gas flaring processes and improve the efficiency of conventional SCPPs. The implementation of numerical models showed that the new design increased the power generation from 50 kW to 788 kW for an SCPP with scales similar to Manzanares. Moreover, studying various locations for gas injections, it was found that the optimum spot is under the collector area and near the inlet section.

Recently, Cuce et al. [152] analyzed the integration of a ground-based waste heat source in an SCPP using a 3D CFD model based on the Manzanares pilot plant. Their results showed that a 250 °C heat source increased power output from 54.14 kW to 129.28 kW at 1000 W/m^2 solar radiation, while up to 101.52 kW could still be generated during periods without solar radiation. The study highlights the potential of waste heat integration to significantly improve SCPP performance and maintain electricity generation during low-solar or nighttime conditions.

4.10. Integration with hydrogen production systems

Abdelsalam et al. [153] proposed a system that integrates an electrolyzer with an SCPP for hydrogen production, with the electrolysis equipment located at the base of the solar chimney (Fig. 32). The results indicated that weather conditions significantly influenced the performance of the SCPP. Additionally, the oxygen produced as a byproduct could be utilized in various industries. Overall, the SCPP, with its hydrogen production capabilities, offers an efficient and sustainable solution for storing excess renewable energy.

Shariatzadeh et al. [154] introduced an innovative power plant design that incorporates an SCPP, solid oxide fuel cells (SOFCs), and

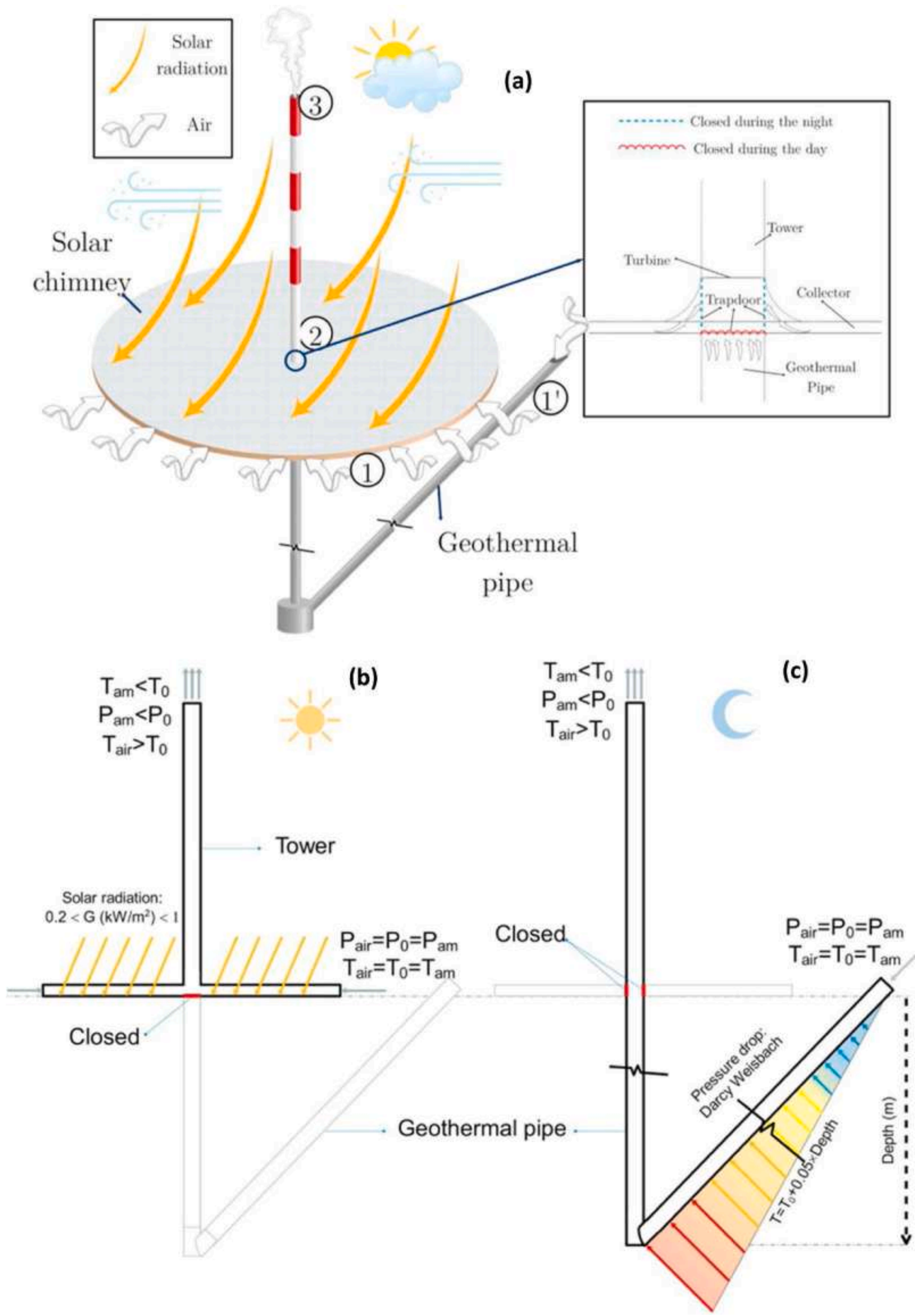

Fig. 28. The integration of a geothermal pipe with an SCPP; (a) the entire combined structure, (b) the daytime working process, (c) the nighttime working process [139].

solid oxide electrolysis cells (SOECs) to address the challenge of insufficient electricity generation from solar chimneys at night. The solar chimney operates during the day to generate electricity, and any excess energy produced is utilized to produce hydrogen in the electrolysis station. This stored hydrogen can then be converted back into electricity using SOFCs during nighttime when solar energy is unavailable. A study conducted in a district of El Paso, Texas, known for its high solar radiation, demonstrated that this system could meet 79.26 % of the energy demand in summer and 37.04 % in winter.

In their study, Fei et al. [155] optimized the configuration of a hybrid SCPP integrated with a SOFC and a SOEC for application in a region of Kerman. The optimization results indicated a greater need for backup electricity in winter. On February 1, electricity generation between 8:30 and 16:00 surpassed demand, while on July 30, this occurred between 5:30 and 17:50, allowing surplus energy to be stored for use when demand exceeds generation.

Jemal et al. [156] investigated a hybrid solar chimney system capable of simultaneously producing electricity and green hydrogen by

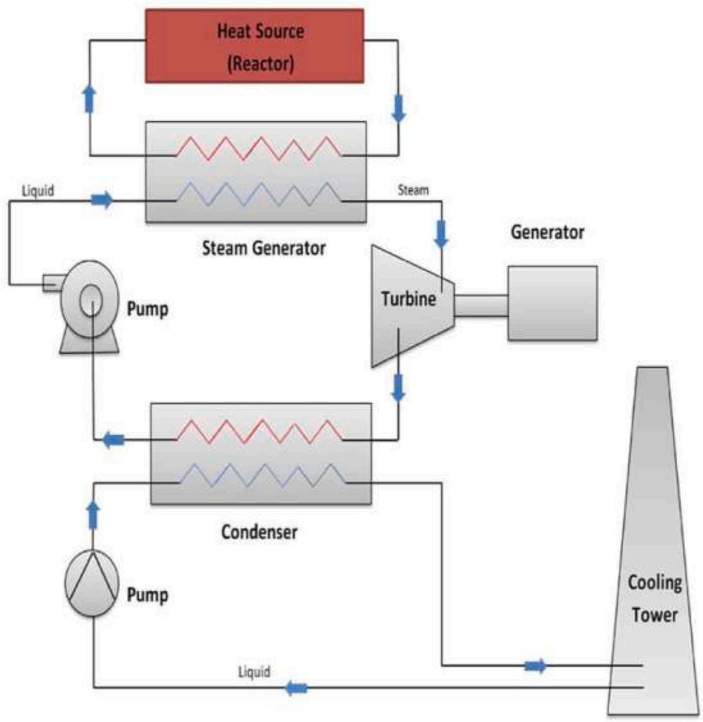

Fig. 29. Schematic of the proposed combined solar-nuclear cycle by Fathi et al. [14].

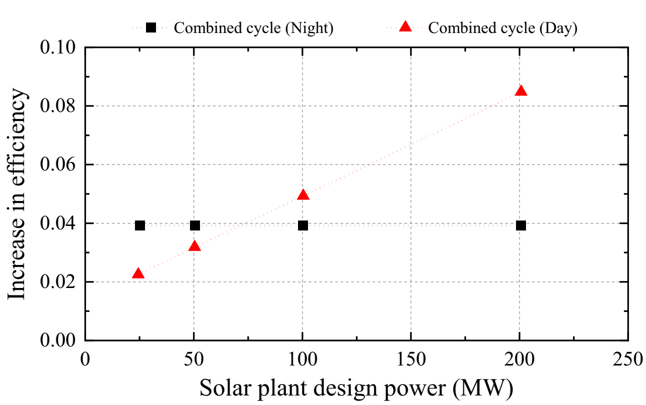

Fig. 30. Increase in efficiency of the combined solar-nuclear cycle [14].

integrating an electrolysis unit with the SCPP. Using CFD simulations combined with Pearson correlation analysis, analytic hierarchy process (AHP), and k-means clustering, they optimized key operating parameters such as chimney inclination, solar radiation, collector absorptivity, and turbine pressure drop. The optimal configuration was obtained at a chimney inclination of 8°, solar radiation of 800 W/m^2, collector absorptivity of 0.88, and a turbine pressure drop of 95 Pa, yielding an airflow velocity of 9.8 m/s, electrical power output of 16.1 kW, and hydrogen production of 0.62 kg/day. The study demonstrated that appropriate aerodynamic and thermal optimization of SCPP systems can significantly enhance both electricity generation and hydrogen production in integrated renewable energy systems.

It should be noted that the papers referenced in this section explore the integration of hydrogen generation and storage with SCPP structures to level out energy production of the SCPPs over time periods where power generation is not stable, such as the day-night cycle or seasonal variations in solar radiation intensity. These technologies do not represent improvements to the design or function of the SCPPs themselves, and hydrogen production/storage facilities would serve the exact same purpose when used in conjunction with other fluctuating renewable sources, such as PV solar or wind turbines. As such, the integration of hydrogen technology does not constitute a direct advantage to SCPPs in comparison to other renewables, but does help to mitigate the shortcomings of some green power generation technologies compared to fossil fuel sources and nuclear.

4.11. Integration with nuclear district heating and cooling systems

Integration of the SCPP with district heating and cooling systems could lead to a more economical hybrid system. A typical district heat profile is illustrated in Fig. 33 shows that most of the time, the demand is much lower than the peak, which means extra heat supply is available to be employed. Considering the growing interest in nuclear heat-only reactor technologies (such as Teplator, or the Chinese DHR-400), which are under development for low-cost heat generation applications [157,158], a hybrid nuclear heat and SCPP electricity generation system seems beneficial, especially for cold climate countries with mostly cloudy weather. This idea is novel and needs techno-economic evaluation and optimization in future studies.

Although the investigated configurations differ in terms of auxiliary technologies and operating conditions, these studies discussed above consistently demonstrate that integrating solar chimney power plants with complementary systems—such as photovoltaic modules, thermal storage, desalination units, or geothermal heat sources—can enhance the overall functionality of the plant by enabling simultaneous electricity generation and additional useful outputs.

5. Thermal analyses

The operational principle of an SCPP is based on the pressure differential between the interior and exterior of the system, which occurs when the air temperature increases within the collector. This temperature rise generates a buoyancy force that facilitates the upward movement of air through the chimney, where a wind turbine is positioned. As the pressure drop and air flow rate are the two essential factors

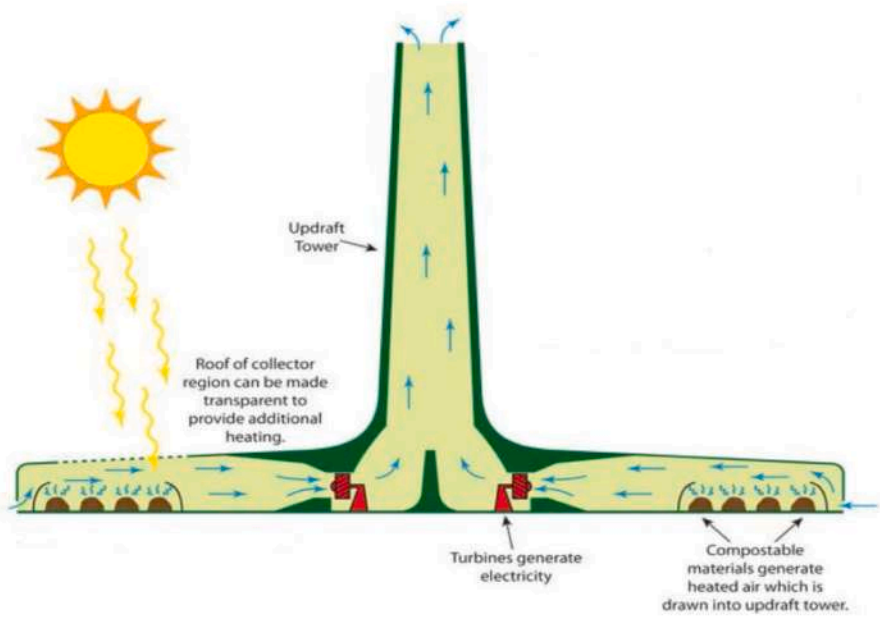

Fig. 31. Hybrid solar-compost waste heat updraft tower (adopted from [142]).

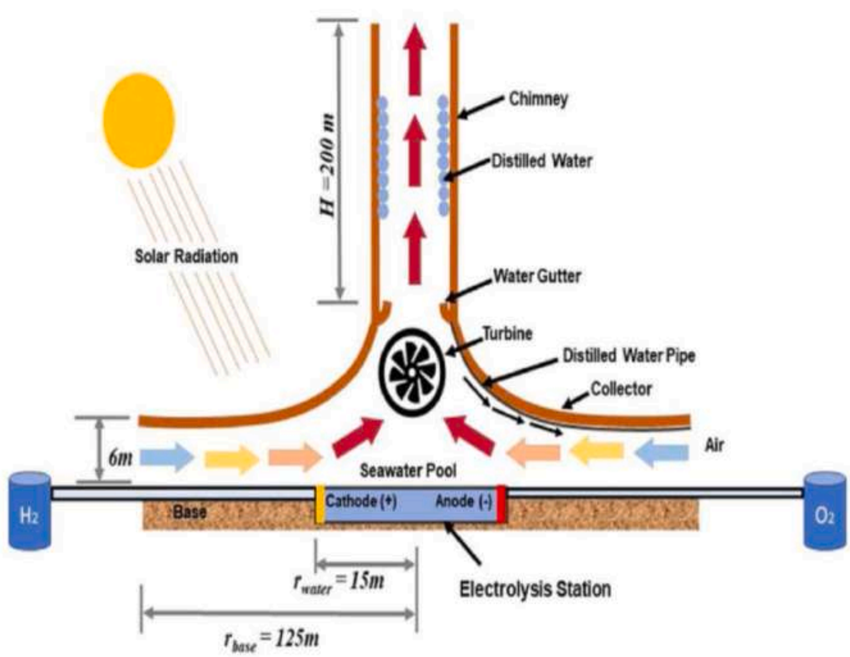

Fig. 32. The SCPP and electrolysis station (adopted from [153]).

determining the SCPP power generation, to design, optimize or analyze the performance of an SCPP, the thermodynamic behavior of the system needs to be modeled. The thermodynamic behavior of the system depends on many variables and parameters such as solar radiation, ambient temperature, the geometry of the system, efficiencies of the equipment, thermal specifications of the used materials, operation scheduling, etc. Due to the complexity of the problem, the developed analytical methods are based on several different simplifications and are widely used to estimate the overall performance of the system [159], and for the verification and validation of numerical simulations [160].

The steady-state driving force, i.e., the pressure drop through the chimney (Δp) is calculated as a function of the SCPP's geometric parameters and fluid specifications as given in Eq. (2) assuming convective flow and neglecting flow viscosity. Also, the overall maximum driving power in the absence of the turbine is given in Eq. (3) [67].

$$\Delta p_{tot} = \left(\frac{g^2}{2c_p}\right)^{\frac{1}{3}} \cdot \left(\frac{{\rho_0}^2{\beta_0}^2}{\rho}\right)^{\frac{1}{3}} \cdot \left(\frac{H_t}{{R_t}^2}\right)^{\frac{2}{3}} .{R_c}^{4/3}.q^{2/3} \quad (2)$$

$$\mathrm{P}_{max} = \frac{\rho_0}{\rho}\frac{\pi g}{c_p T_0} H_t {R_c}^2 q \quad (3)$$

where g(m/s^2) is acceleration due to gravity, c_p is the specific heat (J/kg. K), R_t and H_t are the radius and height of the chimney tower, respectively, and R_c is the circular shape collector's radius. The term q represents the captured solar radiation by the collector (W/m^2), and β

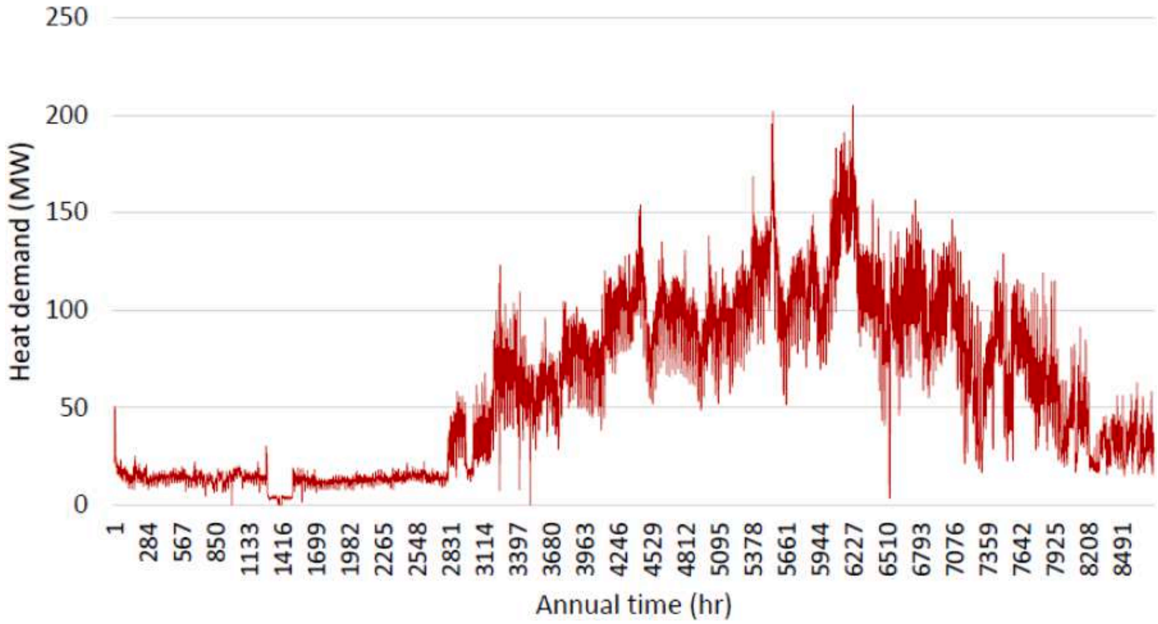

Fig. 33. A typical district heating demand profile [180].

denotes the volume coefficient of expansion. T_0 and ρ_0 are the environmental air temperature and density, respectively [67].

When a turbine is added to the system, the pressure drop over the chimney is distributed into two terms: dynamic pressure losses (associated with the kinetic energy losses of airflow exiting the chimney) and turbine pressure drop, as given in Eq. (4), neglecting the other kinds of pressure losses, such as friction loss [161].

$$\Delta p_{tot} = \Delta p_{turb} + \Delta p_{dyn} \tag{4}$$

Since dynamic pressure affects the airflow rate (Eqs. (4) and (5)), it consequently governs the turbine power generation (Eq. (6)). Therefore, a trade-off exists between the dynamic and turbine pressure drops. The electrical power generated by the turbine can be determined using Eq. (6) [161].

$$\dot{m} = \frac{\pi g \beta_0 \rho_0 q}{c_p \Delta p_{tot}} H_t R_c^{\,2} \tag{5}$$

$$P = \frac{\eta_{turb} \Delta p_{turb} \dot{m}}{\rho} \tag{6}$$

where Δp_{turb} is the pressure drop across the turbine, $\dot{m}$ is the mass flow rate of air passing through the turbine, and η_{turb} is the turbine energy conversion efficiency. Several studies examined the optimum turbine pressure based on different simplifying assumptions. As an example, when the available total pressure drop in the system is assumed to be constant, extracting 2/3 of the total pressure drop by the turbine is the optimum operation, leading to a maximum power generation [161].

Fathi et al. [160], developed an analytical steady-state 1D mathematical model by neglecting the friction losses and the heat storage behavior of the ground. The average amounts of air density and temperature were considered for the pressure drop calculations in the collector, tower, and turbine, considering constant specific heat capacity for the air. In another study, an analytical 1D unsteady model with an hourly operation-based model was proposed by Guo et al. [162], where the model was solved using numerical calculations. The heat storage behavior of a soil layer located under the collector and its effect on the performance and operation of the system was investigated, finding that high specific heat capacity and thermal conductivity of soil helped to smooth the output power over the day. The study considered uniform heating of the ground and neglected the effect of the altitude angle of the sun, while assuming constant density, specific heat capacity and thermal conductivity for the heat storage under the collector [163]. Choi et al. [163] developed a 1D analytical model for estimating the steady-state output power of SCPPs, considering the behavior of water heat storage under the collector, and including the solar radiation and friction pressure losses in the collector. The problem was solved using an iterative algorithm coded and simulated in MATLAB.

For a detailed investigation of the flow characteristics over the entire system, the CFD-based analyses have been widely used [164]. The governing equations, including the conservation of mass, momentum, and energy (Eqs. (7)-(9)), need to be solved to predict the detailed flow and heat transfer characteristics inside the SCPP. The partial differential governing equations modeling the thermodynamic characteristics of fluid were obtained in two forms: conservation form and non-conservation form. The conservation form was derived from applying fundamental physical principles for an infinitesimal volume control fixed in space and the fluid moving through it (Fig. 34a). The non-conservation form was derived from applying fundamental physical principles for a moving infinitesimal volume control of the fluid inside the general flow (Fig. 34b) [165].

The conservation form of the governing equations, given in Eqs. (7)-(9) [165] is the most popular one in CFD.

$$\frac{\partial \rho}{\partial t} + \sum_{i=1}^{d} \frac{\partial (\rho u_i)}{\partial x_i} = 0 \tag{7}$$

$$\frac{\partial (\rho u_i)}{\partial t} + \sum_{j=1}^{d} \frac{\partial (\rho u_i u_j)}{\partial x_j} = -\frac{\partial p}{\partial x_i} + \sum_{j=1}^{d} \frac{\partial \tau_{ij}}{\partial x_j} + \rho f_i, \; i, \; j : X, \; Y, \; Z \tag{8}$$

$$\frac{\partial E}{\partial t} + \sum_{i=1}^{d} \frac{\partial (E u_i)}{\partial x_i} = \sum_{i=1}^{d} \rho f_i u_i + \sum_{i,\, j=1}^{d} \frac{\partial (\tau_{ij} u_i)}{\partial x_j} + \rho q - \sum_{i=1}^{d} \frac{\partial q_i}{\partial x_i}$$

$$q_i = -K \frac{\partial T}{\partial x_i} \tag{9}$$

$$E = e + \frac{V^2}{2}$$

$$e = c_V T \tag{10}$$

In these equations, ρ is the flow density, u_i is the i-component of flow velocity in direction (e.g., x, y, z), p is the pressure distribution acting on

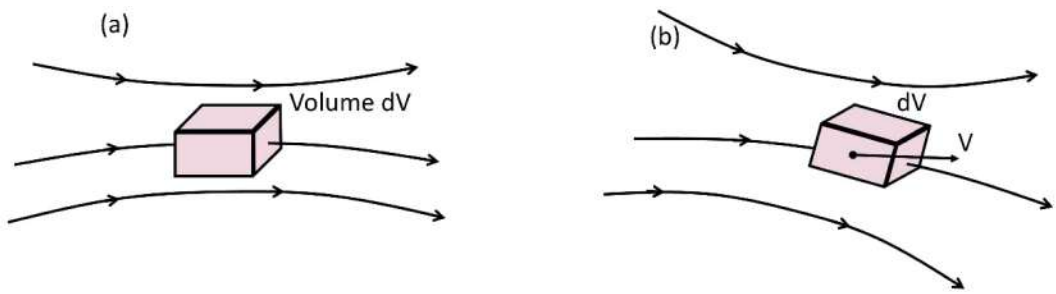

Fig. 34. Two control volume approaches (adapted from [165]). (a) shows the conservation form driven by applying fundamental physical principles for an infinitesimal volume control fixed in space and the fluid moving through it. (b) shows non-conservation form driven by applying fundamental physical principles for moving infinitesimal volume control of the fluid inside the general flow.

the surface of a fluid element from surrounding elements, f_i is the i-component of body force per unit mass acting "at a distance" on a fluid element, e.g., gravitational force. τ_{ij} denotes stress in the j-direction exerted on a plane perpendicular to the i-axis. E is the total energy (internal energy, e, plus kinetic energy, $\frac{V^2}{2}$, per unit mass), and q is the heat transfer rate (emission or absorption) by thermal conduction, proportional to the local temperature gradient, where the thermal conductivity is denoted by K. Here, we have five equations for six unknown flow-field variables; therefore, at least one more constitutive equation modeling a thermodynamic relation between the state variables of the system is required to close the entire system. For example, Eq. (10) represents an equation for a calorically perfect gas, where the internal energy is proportional to the temperature, and c_V is the specific heat at constant volume. Applying the boundary conditions and initial conditions of a specific system to the equations provides the solutions [165].

As the Rayleigh number in SCPPs is large (mostly $Ra>10^{10}$), the flow is turbulent [166]. RANS (Reynolds-averaged Navier-Stokes) models (e.g., k-ε or k-ω) are derived from the Navier-Stokes equations through the decomposition of variables into two components, time-averaged and fluctuating terms. This method is the most suitable option for most engineering turbulent flow CFD calculations, giving approximate time-averaged solutions to the Navier-Stokes formulations [167]. Fathi et al. [160] used a numerical method based on the standard k- ε turbulence model to investigate the Manzanares prototype by comparing the results of the analytical model against CFD calculations.

6. Economic and environmental analyses

Table 5 shows the electricity output and dimensions of the different SCPPs investigated by Schlaich et al. [63,168]. The cost analysis revealed that the levelized cost of electricity (LCOE) would significantly drop by increasing the SCPP size. The estimated LCOE for a 5 MW SCPP was 0.25 €/kWh, while the corresponding value for a 200 MW SCPP was 0.08 €/kWh.

Zhou and Yang [169] estimated the LCOE of an SCPP with a floating chimney in the deserts of China to be about 0.099 $/kWh, competitive with clean coal power plants.

Cost analyses for two different SCPPs with a power output of 100 MW were conducted by Fluri et al. [43,170]. The LCOE was estimated to be in the order of 0.27–0.43 €/kWh. When considering the effect of carbon credits, the LCOE decreased from 0.27 €/kWh to 0.232 €/kWh. Cao et al. [171] performed economic analyses for a conventional and a sloped SCPPs of up to 100 MW. The results suggested that the sloped SCPP was more cost-effective than the conventional one. The initial estimated cost for the sloped SCPP of 100 MW was 29 % lower than that of a similar conventional SCPP. The economic feasibility of a combined system of SCPP and water distillation plant was carried out by Abdelsalam et al. [126]. The estimated LCOE for the combined system was reported as 1.86 $/kWh. The LCOE dropped by increasing the chimney

Table 5
Investment cost and levelized cost of electricity (LCOE) for four different solar chimney power plants [168].

Capacity	MW	5	30	100	200
Tower cost	Million €	19	49	156	170
Collector cost	Million €	13	59	131	318
Turbine cost	Million €	8	32	75	133
Engineering, tests, misc.	Million €	5	16	40	42
Total	Million €	45	155	402	662
LCOE	€/kWh	0.25	0.12	0.10	0.08

height due to an enhancement in solar chimney efficiency. However, this improvement in the LCOE was reduced by the extra capital and operational costs of an SCPP with a taller chimney. Li et al. [172] performed cost-benefit analyses of a 100 MW reinforced concrete SCPP in four different phases during its assumed service period of 120 years (each phase comprises 30 years). Table 6 illustrates the estimated minimum electricity price for each phase with and without carbon credit. The minimum electricity prices in phases 2 to 4 are compatible with current market prices.

The efficiency and cost analysis of a wind-supercharged SCPP was carried out by Zuo et al. [173]. A wind-supercharged SCPP is established by putting an unpowered wind pressure wheel at the chimney top. At the speed of 100 rpm, the shaft power of a conventional SCPP was 37.8 kW, while the wind-supercharged SCPP had a shaft power of 57.03 kW. The estimated electricity price of the wind-supercharged SCPP was 0.216 $/kWh, while that of the conventional SCPP was estimated at 0.27 $/kWh. Bhuiyan et al. [174] performed the economic analysis on a 100 MW floating chimney power plant while comparing the obtained results with the cost-benefit of a conventional concrete solar chimney power plant. The results suggested that the floating chimney power plant had a lower LCOE. The estimated LCOE of the floating SCPP was 0.043 $/kWh compared to 0.184 $/kWh for the concrete SCPP.

To address the environmental impacts of SCPPs, van Blommestein and Mbohwa [175] conducted a life cycle assessment on a 1MW SCPP with a lifespan of 30 years and a construction period of 3 years. Results indicated that Copper and Chromium are the materials which require the most energy to produce for the construction of an SCPP (referred to in the paper as a "power tower"). Coal power had a significant role in producing energy to construct the SCPP, especially in the refinement of

Table 6
Estimated minimum electricity price for each phase in the service period of a 100 MW reinforced concrete solar chimney power plant [172].

Phase	Min. Electricity price $/kWh, with carbon credit	Min. Electricity price $/kWh, without carbon credit
1	0.16	0.17
2	0.01	0.017
3	0.0064	0.013
4	0.0032	0.01

the copper and chromium. Therefore, the consumption of coal leads to the majority of CO_2 and NOx emissions associated with SCPP construction. A solution is to use natural gas or nuclear power to minimize coal consumption and reduce CO_2 and NOx. Salameh et al. [176]. proposed a novel hybrid SCPP associated with an RO water desalination unit for electricity and water production. Analytical results revealed that the RO integration of an SCPP could reduce the CO_2 emission by 361 tons, while if the RO unit uses conventionally sourced electricity, the CO_2 emission increases by 459 tons. Pretorius [177] investigated the effects of vegetation under the collector roof on the temperature lapse rate. He reported that when the vegetation is treated with sufficient water, it will survive under the collector roof, and the inclusion of vegetation will bring a major sacrifice in the plant's performance. Xu and Zhou [178] conceptualized the co-production of power and vegetation in a modified SCPP to answer whether the advantages of vegetation outweigh the disadvantages associated with the reduced power output. Numerical results exhibited that as the vegetation area expanded, the power output reduced while the mass flow rate of the vapor evaporating from the vegetation area rose. Furthermore, higher humidity of ambient air reduced the mass flow rate of vapor evaporating from the vegetation area and consequently increased the collector temperature rise, total pressure potential, and the air mass flow rate, leading to enhanced power production. Finally, they concluded that the benefit from agricultural products was larger than the loss caused by the reduced electricity generation. Hachicha et al. [179] proposed a unique concept by integrating an air filtration unit with SCPPs and studied possible integration locations to optimize the system operation. Numerical data indicated that when the filter is positioned inside the chimney, a considerable pressure drop occurs for the airflow, reducing the air velocity and power generation. However, when the filter is positioned close to the inlet of the collector, the induced pressure drop is reduced, where the rise in velocity is recovered as the air moves toward the chimney. Moreover, the filter efficiency increases from 53.73 % to 89.67 % by changing the filter location from the chimney to the collector area, at the expense of increasing the cost of the filter from 4.83 to $ 7.53 million. This study puts forth the dual functionality of future SCPPs for mitigating urban air pollution and generating electricity simultaneously.

7. Conclusions

Solar chimney power plants (SCPPs) represent a promising renewable energy technology capable of converting low-grade solar thermal energy into electricity through a relatively simple buoyancy-driven mechanism. This review has examined the technological evolution and recent advancements in SCPP systems over the past two decades, focusing on the main engineering strategies proposed to enhance system performance and improve economic feasibility.

One of the most extensively studied approaches involves geometrical optimization of the solar chimney system, including modifications to chimney height, chimney divergence angle, collector diameter, collector roof inclination, and absorber configurations. The reviewed studies consistently demonstrate that increasing chimney height and collector size enhances the buoyancy-driven airflow and improves turbine power output, although these improvements often come with increased construction costs. Novel geometrical concepts such as diffuser chimneys, double-chimney configurations, inflatable towers, floating chimneys, and wavy absorber designs have also been proposed to improve aerodynamic performance or reduce structural costs.

Turbine design and performance optimization represent another critical factor affecting SCPP efficiency. Since a significant portion of the system pressure drop occurs across the turbine, improvements in turbine blade geometry, pressure-drop optimization, and multi-turbine configurations can significantly increase energy extraction efficiency. Advanced turbine concepts, including counter-rotating turbines and vortex-based energy harvesters, have been investigated to enhance energy conversion within the chimney section.

The review also highlights the importance of collector and absorber innovations, including improvements in glazing materials, absorber surfaces, and ground heat storage strategies. Modifications to collector materials, the use of alternative absorber materials, and the integration of thermal storage media such as gravel, water, or phase change materials have demonstrated potential to improve heat absorption and reduce power fluctuations during nighttime operation.

In recent years, research has increasingly focused on hybrid solar chimney systems, where SCPPs are integrated with other renewable or industrial energy systems to enhance overall performance and expand their applications. These hybrid concepts include combinations with photovoltaic systems, solar concentrators, geothermal resources, thermal energy storage units, desalination plants, and waste-heat recovery systems. In addition, emerging concepts such as building-integrated solar chimneys and hybrid SCPP-hydrogen production systems demonstrate the flexibility of solar chimney technology and its potential integration into future sustainable energy infrastructures.

Despite these technological advancements, several challenges still limit the widespread commercialization of SCPP technology. The relatively low conversion efficiency, large land requirements, and high capital costs associated with large chimney structures remain the primary barriers to large-scale deployment. However, ongoing research focusing on hybridization, advanced materials, improved turbine technologies, and innovative structural concepts indicates that solar chimney systems may become more economically competitive in the future.

Overall, the literature reviewed in this study demonstrates that SCPP technology continues to evolve through innovative engineering solutions and interdisciplinary system integrations. Continued research addressing the technical, economic, and environmental aspects of SCPP systems will be essential for improving their performance and enabling their practical implementation as part of the global transition toward sustainable energy systems.

8. Perspectives and critical research gaps

Solar chimney power plants are a rare solar thermal power technology that does not rely on water for energy production and could be a favorable alternative to concentrating solar power systems, especially for remote areas where water availability is an issue. Recent investigations have proved the adaptability of SCPP technology to urban areas, although this concept is still in its early stages. In this regard, miniaturization of such plants is necessary, and more studies are needed to provide a general and comprehensive model for integrating SCPP into commercial and residential buildings.

For improving the techno-economic aspects of SCPP technology, several studies have investigated the potential benefits of integrating SCPP with other technologies. For instance, applying solar reflectors to small-scale SCPPs has shown promising potential for performance enhancement with up to a 57 % rise in output power. However, the number of works concerning this topic is very scarce, and more research and development must be carried out to assess other types of reflectors and provide a better outlook. The synergy effect between PV and SCPP is an important factor that improves the chimney performance and increases the PV efficiency, leading to a highly efficient co-generative power plant. The photovoltaic panels could be used as both the roof cover and collector absorber; however, the offset between the temperature rise on the cell surface and the heat gain should be considered in determining the optimum integration design. The literature currently lacks studies on the integration of concentrating PV systems with SCPP, despite the potential for this combination to result in higher temperature gradients and thereby enhanced output power generation. Moreover, Luminescent solar concentrators (LSCs), similar to PV-SCPPs, can be used as collector covers, providing promising prospects for further growth and development in co-generative power plants. However, they remain one of the underexplored technologies associated with SCPPs.

Since SCPPs are usually built on a large scale, the space inside the solar collector has a microclimate very similar to that of a greenhouse, and it provides an excellent opportunity for crop production, especially in locations with land constraints. The limited studied cases in this field were mostly focused on the vegetation effects on power generation and have not covered the agronomical part. As a result, the suitable types of crops, cultivation patterns, and watering systems have remained unknown, and future research should address these topics. Furthermore, the combination with current emerging technologies, such as Agrivoltaics, has the potential to foster a novel sustainable system with a triple-production concept, paving the way for the commercialization of SCPPs.

As the integration of solar chimney mechanisms with solar dryers has promoted drying efficiency to some extent, the combination of SCPPs with large industrial drying systems could also be beneficial if the quality of dried materials is not negatively affected by air and the harsh environment. Thus, several feasibility studies must be conducted to address the suitability of drying temperature, air and dried material qualities, and the optimum installation of drying trays under the collector roof area.

Although the life cycle assessment (LCA) studies are rare and old, primary LCA analyses have demonstrated that copper consumption is a major concern, accounting for more than 45 % of total CO_2 emissions in the material production process. Therefore, investigations with a detailed approach are needed to clarify the potential spots for material selection and environmental improvements. For instance, the application of sustainable materials for SCPP structure using biodegradable materials could be of interest in this topic.

Dust deposition is a significant challenge in SCPPs and could be a limiting factor in choosing the collector cover material. So far, no specific study has been devoted to the dust and pollution deposition impacts and strategies for removal, and this should be further addressed. The development of new nano-coatings or dust-resistant cover materials for the collector roof can also be investigated in future research to reduce the risk of salt deposition and pave the way for offshore applications.

Another factor influencing the economic viability of SCPPs is the cost of freshwater locally. Many areas lacking natural freshwater resources rely on desalination to meet the growing demand of their population. Regions such as the Middle East and Australia have suitable geography and climate for SCPP construction, and rely heavily on desalination for freshwater production. The integration of desalination technologies to SCPPs may increase the revenue of the plant, thereby lowering effective LCOE enough to compete with PV solar or wind turbines, which cannot produce freshwater directly.

Therefore, addressing the following gaps will improve performance, reliability, and sustainability, supporting wider adoption and technological progress of SCPPs.

- Urban Miniaturization and Integration: There is limited modeling and feasibility data on SCPP systems for commercial and residential urban applications.
- Solar Reflectors and Concentrators: Optimal types and configurations for performance enhancement require more detailed experimental and comparative analysis.
- Advanced Hybridization Technologies: Integration of concentrating PV systems and luminescent solar concentrators with SCPPs remains largely unexplored.
- Agronomical Aspects in SCPP-Greenhouse Hybrids: Suitability of crops, cultivation patterns, and irrigation for SCPP-greenhouse synergy needs further study.
- Industrial Drying System Integration: Feasibility and technical benefits of combining SCPPs with large-scale drying systems in agriculture and industry are insufficiently researched.
- Material Sustainability and Environmental Impact: Life cycle assessments, especially related to copper consumption and use of sustainable or biodegradable materials, are rare.
- Dust and Pollution Management: Research specifically on dust and pollution deposition impacts on collector covers, removal strategies, and nano-coatings is currently lacking.

CRediT authorship contribution statement

Hossein Ebadi: Data curation, Formal analysis, Writing – review & editing. **Sepideh Maleki:** Data curation, Writing – review & editing. **Christopher George:** Writing – review & editing. **Maryam Haghsheno:** Writing – review & editing. **Seyed Sobhan Aleyasin:** Data curation, Formal analysis, Methodology, Project administration, Supervision, Writing – original draft, Writing – review & editing. **Laura Savoldi:** Writing – review & editing, Supervision, Data curation. **Nima Fathi:** Writing – review & editing, Writing – original draft, Methodology, Funding acquisition, Conceptualization, Project administration, Supervision.

Declaration of competing interest

The authors declare that they have no known competing financial interests or personal relationships that could have appeared to influence the work reported in this paper.

Data availability

Data will be made available on request.

References

[1] "World Resources Institute," *WRI*. https://www.wri.org/data/world-greenhouse-gas-emissions-2019.

[2] M. Filonchyk, M.P. Peterson, L. Zhang, V. Hurynovich, Y. He, Greenhouse gases emissions and global climate change: examining the influence of CO_2, CH_4, and N_2O, Sci. Total. Environ. 935 (2024) 173359, https://doi.org/10.1016/j.scitotenv.2024.173359.

[3] S. Gorjian, H. Ebadi, L.D. Jathar, L. Savoldi, Chapter 1 - solar energy for sustainable food and agriculture: developments, barriers, and policies, in: S. Gorjian, P.E. Campana (Eds.), Solar Energy Advancements in Agriculture and Food Production Systems, Academic Press, 2022, pp. 1–28, https://doi.org/10.1016/B978-0-323-89866-9.00004-3.

[4] IEA. (2024), "Renewables 2024," Paris, https://www.iea.org/reports/renewables-2024.

[5] *Renewable Energy Market update*. OECD, 2020, https://www.iea.org/reports/renewable-energy-market-update.

[6] World Energy Outlook 2021, Int. Energy Agency (2021). https://www.iea.org/reports/world-energy-outlook-2021.

[7] D. Lerede, L. Savoldi, Might future electricity generation suffice to meet the global demand? Energy Strateg. Rev. 47 (2023) 101080 https://doi.org/10.1016/j.esr.2023.101080.

[8] International data - electricity, U.S Energy Inf. Administ. (2021). https://www.eia.gov/international/data/world/electricity/electricity-generation.

[9] S. Gorjian and H. Ebadi, "Chapter 1 - Introduction," S. Gorjian and A. B. T.-P. S.E. C. Shukla, eds. Academic Press, 2020, pp. 1–26, https://doi.org/10.1016/B978-0-12-819610-6.00001-6.

[10] P. Breeze, "Chapter 13 - solar Power," P. B. T.-P. G. T. (Third E. Breeze, Third ed. Newnes, 2019, pp. 293–321, https://doi.org/10.1016/B978-0-08-102631-1.00013-4.

[11] R. Pitz-Paal, "19 - Concentrating solar Power," T. M. B. T.-F. E. E. Letcher, Third ed. Elsevier, 2020, pp. 413–430, https://doi.org/10.1016/B978-0-08-102886-5.00019-0.

[12] S. Gorjian, F. Kamrani, H. Ebadi, S. Samanta, and L. Savoldi, "Chapter 25 - applications of renewable energy sources in agriculture from a complementarity perspective," J. Jurasz and A. B. T.-C. of V. R. E. S. Beluco, Eds. Academic Press, 2022, pp. 615–647, https://doi.org/10.1016/B978-0-323-85527-3.00019-4.

[13] C.B. Maia, J. de O. Castro Silva, Thermodynamic assessment of a small-scale solar chimney, Renew. Energy 186 (2022) 35–50, https://doi.org/10.1016/j.renene.2021.12.128.

[14] N. Fathi, et al., Efficiency enhancement of solar chimney power plant by use of waste heat from nuclear power plant, J. Clean. Prod. 180 (2018) 407–416, https://doi.org/10.1016/j.jclepro.2018.01.132.

[15] W. Haaf, K. Friedrich, G. MAYR, J. Schlaich, Part I: principle and construction of the pilot plant in Manzanares, Int. J. Sol. Energy 2 (1) (1983) 3–20, https://doi.org/10.1080/01425918308909911.

[16] W. Haaf, Part II: preliminary test results from the Manzanares Pilot Plant, Int. J. Sol. Energy 2 (2) (1984) 141–161, https://doi.org/10.1080/01425918408909921.

[17] M.M. Padki, S.A. Sherif, On a simple analytical model for solar chimneys, Int. J. Energy Res. 23 (4) (1999) 345–349, https://doi.org/10.1002/(SICI)1099-114X(19990325)23:4<345::AID-R485>3.0.CO;2-Z.
[18] T. Chitsomboon, The effect of chimney top convergence on efficiency of a solar chimney, in: Proceedings of the 13th National Mechanical Engineering Conference, Pataya, Thailand, 1999, pp. 263–268.
[19] A.J. Gannon, T.W. Von Backström, Solar chimney cycle analysis with system loss and solar collector performance, J. Sol. Energy Eng. Trans. ASME 122 (3) (2000) 133–137, https://doi.org/10.1115/1.1314379.
[20] J. Schlaich, The Solar Chimney, Edition Axel Menges, Stuttgart, Germany, 1995. https://books.google.co.in/books?id=CVy6Nh57MdMC&printsec=frontcover&utm.
[21] J.P. Pretorius, D.G. Kröger, Sensitivity analysis of the operating and technical specifications of a solar chimney power plant, J. Sol. Energy Eng. Trans. ASME 129 (2) (2007) 171–178, https://doi.org/10.1115/1.2711473.
[22] C.B. Maia, A.G. Ferreira, R.M. Valle, M.F.B. Cortez, Theoretical evaluation of the influence of geometric parameters and materials on the behavior of the airflow in a solar chimney, Comput. Fluids. 38 (3) (2009) 625–636, https://doi.org/10.1016/j.compfluid.2008.06.005.
[23] X. Zhou, J. Yang, B. Xiao, G. Hou, F. Xing, Analysis of chimney height for solar chimney power plant, Appl. Therm. Eng. 29 (1) (2009) 178–185, https://doi.org/10.1016/j.applthermaleng.2008.02.014.
[24] X. Zhou, F. Wang, R.M. Ochieng, A review of solar chimney power technology, Renew. Sustain. Energy Rev. 14 (8) (2010) 2315–2338, https://doi.org/10.1016/j.rser.2010.04.018.
[25] H.H. Al-kayiem, O. Chikere, Historic and recent progress in solar chimney power plant enhancing technologies, Renew. Sustain. Energy Rev. 58 (2016) 1269–1292, https://doi.org/10.1016/j.rser.2015.12.331.
[26] A.B. Kasaeian, S. Molana, K. Rahmani, D. Wen, A review on solar chimney systems, Renew. Sustain. Energy Rev. 67 (2017) 954–987, https://doi.org/10.1016/j.rser.2016.09.081.
[27] P. Guo, T. Li, B. Xu, X. Xu, J. Li, Questions and current understanding about solar chimney power plant: a review, Energy Convers. Manage 182 (December 2018) (2019) 21–33, https://doi.org/10.1016/j.enconman.2018.12.063.
[28] A.A.M. Omara, H.A. Mohammed, I. Jabbar, A. Rikabi, M. Ali, A.A.A. Abuelnuor, Performance improvement of solar chimneys using phase change materials: a review, Sol. Energy 228 (August) (2021) 68–88, https://doi.org/10.1016/j.solener.2021.09.037.
[29] F.L. Rashid, et al., Current developments, utilization, and effects of phase-change materials integrated with solar chimney: a comprehensive review, J. Energy Storage 105 (2025) 114684, https://doi.org/10.1016/j.est.2024.114684.
[30] S. Pradhan, R. Chakraborty, D.K. Mandal, A. Barman, P. Bose, Design and performance analysis of solar chimney power plant (SCPP): a review, Sustain. Energy Technol. Assessm. 47 (May) (2021) 101411, https://doi.org/10.1016/j.seta.2021.101411.
[31] O.K. Ahmed, S. Algburi, Z.H. Ali, A.K. Ahmed, H.N. Shubat, Hybrid solar chimneys: a comprehensive review, Energy Reports 8 (2022) 438–460, https://doi.org/10.1016/j.egyr.2021.12.007.
[32] P. Das, C.V. Parvathy, A critical review on solar chimney power plant technology: influence of environment and geometrical parameters, barriers for commercialization, opportunities, and carbon emission mitigation, Environ. Sci. Pollut. Res. (2022) 69367–69387, https://doi.org/10.1007/s11356-022-22623-7.
[33] P. Das, V.P. Chandramohan, Review article A review on solar updraft tower plant technology: thermodynamic analysis, worldwide status, recent advances, major challenges and opportunities, Sustain. Energy Technol. Assessm. 52 (PA) (2022) 102091, https://doi.org/10.1016/j.seta.2022.102091.
[34] S. Mehranfar, A. Gharehghani, A. Azizi, A. Mahmoudzadeh, Comparative assessment of innovative methods to improve solar chimney power plant efficiency, Sustain. Energy Technol. Assessm. 49 (November 2021) (2022) 101807, https://doi.org/10.1016/j.seta.2021.101807.
[35] E. Cuce, P.M. Cuce, S. Carlucci, H. Sen, S. Kumarasamy, Md. Hasanuzzaman and R. Daneshazarian, *Solar Chimney Power Plants: a review of the concepts, designs and performances*. 2022, https://doi.org/10.3390/su14031450.
[36] L. Zhu, A.I. Khdair, A. Aghaei, K. Zalipour, H. Chen, M. Afrand, A comprehensive review of solar chimney power plants: technology, performance, and future prospects, Sustain. Energy Technol. Assessm. 81 (104413) (2025), https://doi.org/10.1016/j.seta.2025.104413. Art. no.
[37] D.K. Mandal, K.K. Gupta, N. Biswas, N.K. Manna, S. Santra, A.C. Benim, Optimization of hybrid solar chimney power plants (HSCPPs): a review of multi-objective approaches, Appl. Energy 396 (126214) (2025), https://doi.org/10.1016/j.apenergy.2025.126214. Art. no.
[38] F. Kassaei, A. Bagherzadeh, M. Abedi, A. Bénard, Experimental studies of solar chimneys: a survey of performance, design, and applications for power generation, Energies. (Basel) 18 (17) (2025), https://doi.org/10.3390/en18174634. Art. no. 4634.
[39] A. Koonsrisuk, “Analysis of flow in solar chimney for an optimal design purpose,” Suranaree University of Technology, India, 2009.
[40] J. Schlaich, *The Solar Chimney: electricity from the Sun*, edition ax. Stuttgart, 1995.
[41] S.M. Boualleg, S. Larbi, A. Bouhdjar, D. Amokrane, and A. So, “Influence of environment and aging materials on the performance of solar chimney power plants,” vol. 11, 2021, https://doi.org/10.1051/rees/2021013.
[42] J.P. Pretorius, D.G. Kröger, Critical evaluation of solar chimney power plant performance, Sol. Energy 80 (5) (2006) 535–544, https://doi.org/10.1016/j.solener.2005.04.001.
[43] T.P. Fluri, T.W. Von Backström, Performance analysis of the power conversion unit of a solar chimney power plant, Sol. Energy 82 (11) (2008) 999–1008, https://doi.org/10.1016/j.solener.2008.05.001.
[44] J. Schlaich, R. Bergermann, W. Schiel, G. Weinrebe, Design of commercial solar tower systems - utilization of solar induced convective flows for power generation, in: International Solar Energy Conference, 2003, pp. 573–581, https://doi.org/10.1115/ISEC2003-44057.
[45] E. Cuce, A. Saxena, P.M. Cuce, H. Sen, S. Guo, K. Sudhakar, Performance assessment of solar chimney power plants with the impacts of divergent and convergent chimney geometry, Int. J. Low-Carbon Technol. 16 (3) (Sep. 2021) 704–714, https://doi.org/10.1093/ijlct/ctaa097.
[46] S. Hu, D.Y.C. Leung, Mathematical modelling of the performance of a solar chimney power plant with divergent chimneys, Energy Procedia 110 (2017) 440–445, https://doi.org/10.1016/j.egypro.2017.03.166.
[47] H. Hoseini, R. Mehdipour, Evaluation of solar-chimney power plants with multiple-angle collectors, J. Comput. Appl. Res. Mech. Eng. 8 (1) (2018) 85–96, https://doi.org/10.22061/jcarme.2017.2282.1213.
[48] L. Wang, X. Fan, Failure cases of high chimneys: a review, Eng. Fail. Anal. 105 (2019) 1107–1117, https://doi.org/10.1016/j.engfailanal.2019.07.032.
[49] R. Balijepalli, V.P. Chandramohan, K. Kirankumar, Performance parameter evaluation, materials selection, solar radiation with energy losses, energy storage and turbine design procedure for a pilot scale solar updraft tower, Energy Convers. Manage 150 (2017) 451–462, https://doi.org/10.1016/j.enconman.2017.08.043.
[50] I. Cabanyes, Proyecto de Motor Solar, La Energia Eléctrica, Rev. Gen. Electr. y sus Apl. 8 (1903) 61–65.
[51] H. Günther, In Hundert Jahren, Kosmos - Gesellschaft der Naturfreunde, Stuttgart, 1931.
[52] L.B. Mullett, The solar chimney — Overall efficiency, design and performance, Int. J. Ambient Energy 8 (1) (1987) 35–40, https://doi.org/10.1080/01430750.1987.9675512.
[53] M.M. Padki, S.A. Sherif, Solar chimney for medium-to-large scale power generation, in: Proceedings of the Manila International Symposium on the Development and Management of Energy Resources, 1989. January 26-28Manila, Philippines, in *Development and Management of Energy Resources*, Vol. 1, Philippine Association for the Advancement of Science (PhiLAAS), 1989, pp. 432-443.
[54] M.Q. Yan, “Thermo-fluid analysis of solar chimneys, paper presented at American Society of Mechanical Engineers,” 1991.
[55] M.M. Padki, S.A. Sherif, A mathematical model for solar chimneys, in: *Proceedings of the 1992 International Renewable Energy Conference*, in *Renewable Energy: Research and Applications*, University of Jordan, Faculty of Engineering and Technology, Amman, Jordan, 1992, pp. 289–294. Vol. I, Audi, M.S. (Editor)June 22-26.
[56] M.A. Dos Santos Bernardes, R.M. Valle, M.F.B. Cortez, Numerical analysis of natural laminar convection in a radial solar heater, Int. J. Therm. Sci. 38 (1) (1999) 42–50, https://doi.org/10.1016/S0035-3159(99)80015-4.
[57] D.G. Kröger, D. Blaine, Analysis of the driving potential of a solar chimney power plant, South Afr. Inst. Mech. Eng. R D J. 15 (3) (1999) 85–94. http://www.scielo.org.za/scielo.php?script=sci_arttext&pid=S2309-89881999000100005&lng=en&nrm=iso.
[58] D.G. Kröger, J.D. Buys, Radial flow boundary layer development analysis, South Afr. Inst. Mech. Eng. R D J. 15 (3) (1999) 95–102. https://scielo.org.za/scielo.php?lng=es&nrm=iso&pid=S2309-89881999000100006&script=sci_arttext.
[59] A.J. Gannon, T.W. Von Backström, Solar chimney turbine part 1 of 2: design, in: International Solar Energy Conference, 2002, pp. 335–341, https://doi.org/10.1115/SED2002-1070.
[60] A.J. Gannon, T.W. Von Backström, Solar chimney turbine part 2 of 2: experimental results, in: International Solar Energy Conference, 2002, pp. 343–349, https://doi.org/10.1115/SED2002-1071.
[61] A.J. Gannon, T.W. Von Backström, Solar chimney turbine performance, J. Sol. Energy Eng. Trans. ASME 125 (1) (2003) 101–106, https://doi.org/10.1115/1.1530195.
[62] M.A. dos, A. Voß, G. Weinrebe, Thermal and technical analyses of solar chimneys, Sol. Energy 75 (6) (2003) 511–524, https://doi.org/10.1016/j.solener.2003.09.012.
[63] J. Schlaich, R. Bergermann, W. Schiel, G. Weinrebe, Design of commercial solar updraft tower systems - utilization of solar induced convective flows for power generation, J. Sol. Energy Eng. Trans. ASME 127 (1) (2005) 117–124, https://doi.org/10.1115/1.1823493.
[64] T.W. Von Backström, Calculation of pressure and density in solar power plant chimneys, J. Sol. Energy Eng. Trans. ASME 125 (1) (2003) 127–129, https://doi.org/10.1115/1.1530198.
[65] M.A. Serag-Eldin, Computing flow in a solar chimney plant subject to atmospheric winds, in: Proceedings of the ASME Heat Transfer/Fluids Engineering Summer Conference2004, HT/FED 2004 2 B, 2004, pp. 1153–1162, https://doi.org/10.1115/ht-fed2004-56651.
[66] C.F. Kirstein, T.W. Von Backström, D.G. Kröger, Flow through a solar chimney power plant collector-to-chimney transition section, in: International Solar Energy Conference, 2005, pp. 713–719, https://doi.org/10.1115/ISEC2005-76011.
[67] T. Ming, W. Liu, G. Xu, Analytical and numerical investigation of the solar chimney power plant systems, Int. J. Energy Res. 30 (11) (2006) 861–873, https://doi.org/10.1002/er.1191.
[68] J.P. Pretorius and D.G. Kröger, “Thermo-economic optimization of a solar chimney power plant,” 2006, https://www.crses.sun.ac.za/files/studies/

completed-research/JP%20Pretorius%20-%20PhD%20Thesis-2007-02-13.pdf?utm.
[69] J.P. Pretorius, D.G. Kroger, Solar chimney power plant performance, J. Sol. Energy Eng. Trans. ASME 128 (3) (2006) 302–311, https://doi.org/10.1115/1.2210491.
[70] T.W. von Backström, T.P. Fluri, Maximum fluid power condition in solar chimney power plants - an analytical approach, Sol. Energy 80 (11) (2006) 1417–1423, https://doi.org/10.1016/j.solener.2006.04.001.
[71] H. Huang, H. Zhang, Y. Huang, and F. Lu, "Simulation calculation on solar chimney power plant system," 2007, doi: 10.1007/978-3-540-76694-0_216.
[72] A. Koonsrisuk, T. Chitsomboon, Dynamic similarity in solar chimney modeling, Sol. Energy 81 (12) (2007) 1439–1446, https://doi.org/10.1016/j.solener.2007.03.003.
[73] N. Pasumarthi, S.A. Sherif, Experimental and theoretical performance of a demonstration solar chimney model—Part I: mathematical model development, Int. J. Energy Res. 22 (3) (1998) 277–288, https://doi.org/10.1002/(sici)1099-114x(19980310)22:3<277::aid-r380>3.3.co;2-i.
[74] N. Pasumarthi, S.A. Sherif, Experimental and theoretical performance of a demonstration solar chimney model—Part II: experimental and theoretical results and economic analysis, Int. J. Energy Res. 22 (5) (1998) 443–461, https://doi.org/10.1002/(sici)1099-114x(199804)22:5<443::aid-r381>3.3.co;2-m.
[75] N. Mehla, R. Makade, N.S. Thakur, Experimental analysis of a velocity field using variable chimney diameter for solar updraft tower, Int. J. Eng. Sci. Technol. 3 (4) (2011) 3167–3171. https://www.researchgate.net/publication/265007003_Experimental_analysis_of_a_velocity_field_using_variable_chimney_diameter_for_solar_updraft_tower?utm.
[76] M. Najmi, A. Nazari, H. Mansouri, G. Zahedi, Feasibility study on optimization of a typical solar chimney power plant, Heat Mass Transf. und Stoffuebertragung 48 (3) (2012) 475–485, https://doi.org/10.1007/s00231-011-0894-5.
[77] A.M. Elsayed, O.A. Gaheen, M.A. Aziz, Enhancing solar chimney power plant performance through innovative collector curved-guide vanes configurations, Renew. Energy 232 (2024) 121127, https://doi.org/10.1016/j.renene.2024.121127.
[78] M. Ghalamchi, A. Kasaeian, M. Ghalamchi, Experimental study of geometrical and climate effects on the performance of a small solar chimney, Renew. Sustain. Energy Rev. 43 (2015) 425–431, https://doi.org/10.1016/j.rser.2014.11.068.
[79] M.A.K. Lodhi, Application of helio-aero-gravity concept in producing energy and suppressing pollution, Energy Convers. Manage 40 (4) (1999) 407–421, https://doi.org/10.1016/S0196-8904(98)00104-6.
[80] Y.J. Dai, H.B. Huang, R.Z. Wang, Case study of solar chimney power plants in northwestern regions of China, Renew. Energy 28 (8) (2003) 1295–1304, https://doi.org/10.1016/S0960148102002276.
[81] S. Okada, T. Uchida, T. Karasudani, Y. Ohya, Improvement in solar chimney power generation by using a diffuser tower, J. Sol. Energy Eng. Trans. ASME 137 (3) (2015), https://doi.org/10.1115/1.4029377.
[82] P. Das, V.P. Chandramohan, CFD analysis on flow and performance parameters estimation of solar updraft tower (SUT) plant varying its geometrical configurations, Energy Sources, Part A Recover. Util. Environ. Eff. 40 (12) (2018) 1532–1546, https://doi.org/10.1080/15567036.2018.1477881.
[83] K. Milani Shirvan, S. Mirzakhanlari, M. Mamourian, N. Abu-Hamdeh, Numerical investigation and sensitivity analysis of effective parameters to obtain potential maximum power output: a case study on Zanjan prototype solar chimney power plant, Energy Convers. Manage 136 (2017) 350–360, https://doi.org/10.1016/j.enconman.2016.12.081.
[84] A. Hassan, M. Ali, A. Waqas, Numerical investigation on performance of solar chimney power plant by varying collector slope and chimney diverging angle, Energy 142 (2018) 411–425, https://doi.org/10.1016/j.energy.2017.10.047.
[85] E. Gholamalizadeh, M.H. Kim, CFD (computational fluid dynamics) analysis of a solar-chimney power plant with inclined collector roof, Energy 107 (2016) 661–667, https://doi.org/10.1016/j.energy.2016.04.077.
[86] H. Pastohr, O. Kornadt, K. Gürlebeck, Numerical and analytical calculations of the temperature and flow field in the upwind power plant, Int. J. Energy Res. 28 (6) (2004) 495–510, https://doi.org/10.1002/er.978.
[87] A. Koonsrisuk, T. Chitsomboon, Effects of flow area changes on the potential of solar chimney power plants, Energy 51 (2013) 400–406, https://doi.org/10.1016/j.energy.2012.12.051.
[88] V. Putkaradze, P. Vorobieff, A. Mammoli, N. Fathi, Inflatable free-standing flexible solar towers, Sol. Energy 98 (2013) 85–98, https://doi.org/10.1016/j.solener.2013.07.010.
[89] M. Chi, F. Gay-Balmaz, V. Putkaradze, P. Vorobieff, Dynamics and optimal control of flexible solar updraft towers, Proc. R. Soc. A Math. Phys. Eng. Sci. 471 (2173) (2015), https://doi.org/10.1098/rspa.2014.0539.
[90] P. Vorobieff, A. Mammoli, N. Fathi, V. Putkaradze, Freestanding inflatable solar chimney: experiment and theory, Bull. Am. Phys. Soc. (2014) 59. https://archive.aps.org/dfd/2014/h29/6/?utm.
[91] C.D. Papageorgiou, M. Psalidas, S. Sotiriou, Floating solar chimney technology scale analysis, in: Proceedings of the IASTED International Conference on Power and Energy Systems, EuroPES 2011, 2011, pp. 55–59, https://doi.org/10.2316/P.2011.714-052.
[92] C.D. Papageorgiou, Efficiency of solar air turbine power stations with floating solar chimneys, Series Energy Power Syst. (2004) 127–134.
[93] C.D. Papageorgiou, External wind effects on floating solar chimney, Series Energy Power Syst. (2004) 159–163.
[94] D.K. Mandal, N. Biswas, A. Barman, R. Chakraborty, N.K. Manna, A novel design of absorber surface of solar chimney power plant (SCPP): thermal assessment, exergy and regression analysis, Sustain. Energy Technol. Assessm. 56 (2023) 103039, https://doi.org/10.1016/j.seta.2023.103039.
[95] T.P. Fluri, T.W. von Backström, Comparison of modelling approaches and layouts for solar chimney turbines, Sol. Energy 82 (3) (2008) 239–246, https://doi.org/10.1016/j.solener.2007.07.006.
[96] M. Tingzhen, L. Wei, X. Guoling, X. Yanbin, G. Xuhu, P. Yuan, Numerical simulation of the solar chimney power plant systems coupled with turbine, Renew. Energy 33 (5) (2008) 897–905, https://doi.org/10.1016/j.renene.2007.06.021.
[97] S. Nizetic, B. Klarin, A simplified analytical approach for evaluation of the optimal ratio of pressure drop across the turbine in solar chimney power plants, Appl. Energy 87 (2) (2010) 587–591, https://doi.org/10.1016/j.apenergy.2009.05.019.
[98] M.F.C. Esmail, W.M. A-Elmagid, T. Mekhail, I.M. Al-Helal, Case Studies in Thermal Engineering A numerical comparative study of axial flow turbines for solar chimney power plant, Case Stud. Therm. Eng. 26 (December 2020) (2021) 101046, https://doi.org/10.1016/j.csite.2021.101046.
[99] A.M. Elsayed, O.A. Gaheen, M.A. Abdelrahman, M.A. Aziz, An experimental investigation of a solar chimney integrated with a bladeless wind turbine for sustainable energy harvesting, Energy 304 (2024) 132154, https://doi.org/10.1016/j.energy.2024.132154.
[100] O.K. Ahmed, A.S. Hussein, Case Studies in Thermal Engineering new design of solar chimney (case study), Case Stud. Therm. Eng. 11 (December 2017) (2018) 105–112, https://doi.org/10.1016/j.csite.2017.12.008.
[101] Q. Liu, F. Cao, Y. Liu, T. Zhu, and D. Liu, "Design and simulation of a solar chimney PV /T power plant in Northwest China," vol. 2018, 2018, doi: 10.1155/2018/5164174.
[102] S. Jamali, A. Nemati, F. Mohammadkhani, M. Yari, Thermal and economic assessment of a solar chimney cooled semi- transparent photovoltaic (STPV) power plant in different climates, Sol. Energy 185 (April) (2019) 480–493, https://doi.org/10.1016/j.solener.2019.04.073.
[103] M. Alkasrawi, E. Abdelsalam, H. Alnawafah, F. Almomani, M. Tawalbeh, A. Mousa, Integration of solar chimney power plant with photovoltaic for co-cooling, power production, and water desalination, Processes 9 (12) (2021) 1–17, https://doi.org/10.3390/pr9122155.
[104] A.R. Shahreza, H. Imani, Experimental and numerical investigation on an innovative solar chimney, Energy Convers. Manage 95 (2015) 446–452, https://doi.org/10.1016/j.enconman.2014.10.051.
[105] S. Ouédraogo, M. Ousmane, L. Mogmenga, T.S.M. Ky, S. Kam, J. Bathiébo, Experimental study of the airflow in natural convection in an innovative prototype of solar chimney power plant, under climatic conditions in Ouagadougou, Burkina Faso, Indian J. Sci. Technol. 15 (14) (2022) 619–629, https://doi.org/10.17485/IJST/v15i14.1737.
[106] D.K. Khidhir, S.A. Atrooshi, Investigation of thermal concentration effect in a modified solar chimney, Sol. Energy 206 (2020) 799–815, https://doi.org/10.1016/j.solener.2020.06.011.
[107] F.M. Hussain, F.A. Al-Sulaiman, Performance analysis of a solar chimney power plant design aided with reflectors, Energy Convers. Manage 177 (September) (2018) 30–42, https://doi.org/10.1016/j.enconman.2018.09.043.
[108] A. Akbarzadeh, P. Johnson, R. Singh, Examining potential benefits of combining a chimney with a salinity gradient solar pond for production of power in salt affected areas, Sol. Energy 83 (8) (2009) 1345–1359, https://doi.org/10.1016/j.solener.2009.02.010.
[109] X. Zhou, J. Yang, B. Xiao, J. Li, Night operation of solar chimney power system using solar ponds for heat storage, Int. J. Glob. Energy Issues 31 (2) (Jan. 2009) 193–207, https://doi.org/10.1504/IJGEI.2009.023895.
[110] N. Fadaei, A. Kasaeian, A. Akbarzadeh, S.H. Hashemabadi, Experimental investigation of solar chimney with phase change material (PCM), Renew. Energy 123 (2018) 26–35, https://doi.org/10.1016/j.renene.2018.01.122.
[111] F.J. Hurtado, A.S. Kaiser, B. Zamora, Evaluation of the influence of soil thermal inertia on the performance of a solar chimney power plant, Energy 47 (1) (2012) 213–224, https://doi.org/10.1016/j.energy.2012.09.040.
[112] T. Ming, F. Meng, W. Liu, Y. Pan, R. Kiesgen de Richter, Analysis of output power smoothing method of the solar chimney power generating system, Int. J. Energy Res. 37 (13) (2013) 1657–1668, https://doi.org/10.1002/er.2986.
[113] K. Ikhlef, S. Larbi, İ. Üçgül, Experimental study of different thermal storage system effects on the performance of a small prototype solar chimney power plant, Renew. Energy 200 (2022) 516–526, https://doi.org/10.1016/j.renene.2022.09.087.
[114] M.T. Chaichan, H.A. Kazem, Thermal storage comparison for variable basement kinds of a solar chimney prototype in Baghdad-Iraq weathers, Int. J. Appl. Sci. 2 (2) (2011) 12–20. https://www.cscjournals.org/manuscript/Journals/IJAS/Volume2/Issue2/IJAS-33.pdf?utm.
[115] H. Sharon, A detailed review on sole and hybrid solar chimney based sustainable ventilation, power generation, and potable water production systems, Energy Nexus. 10 (2023) 100184, https://doi.org/10.1016/j.nexus.2023.100184.
[116] A. Azad, E. Aghaei, A. Jalali, P. Ahmadi, Multi-objective optimization of a solar chimney for power generation and water desalination using neural network, Energy Convers. Manage 238 (2021) 114152, https://doi.org/10.1016/j.enconman.2021.114152.
[117] L. Zuo, Y. Zheng, Z. Li, Y. Sha, Solar chimneys integrated with sea water desalination, Desalination. 276 (1–3) (2011) 207–213, https://doi.org/10.1016/j.desal.2011.03.052.
[118] L. Zuo, Y. Yuan, Z. Li, Y. Zheng, Experimental research on solar chimneys integrated with seawater desalination under practical weather condition, Desalination. 298 (2012) 22–33, https://doi.org/10.1016/j.desal.2012.05.001.

[119] X. Zhou, B. Xiao, W. Liu, X. Guo, J. Yang, J. Fan, Comparison of classical solar chimney power system and combined solar chimney system for power generation and seawater desalination, Desalination. 250 (1) (2010) 249–256, https://doi.org/10.1016/j.desal.2009.03.007.

[120] L. Zuo, et al., The effect of different structural parameters on wind supercharged solar chimney power plant combined with seawater desalination, Energy Convers. Manage 176 (2018) 372–383, https://doi.org/10.1016/j.enconman.2018.09.044.

[121] E. Abdelsalam, et al., Performance analysis of hybrid solar chimney–power plant for power production and seawater desalination: a sustainable approach, Int. J. Energy Res. 45 (12) (2021) 17327–17341, https://doi.org/10.1002/er.6004.

[122] E. Abdelsalam, "A novel hybrid solar chimney power plant: performance analysis and deployment feasibility," no. April, pp. 3559–3579, 2022, doi: 10.1002/ese3.1240.

[123] L. Zuo et al., "Experimental research on the operation characteristics of solar chimney power plant combined with distillation (SCPPCD)," vol. 326, no. September 2022, doi: 10.1016/j.apenergy.2022.120029.

[124] C. Mendez and Y. Bicer, "Integrated system based on solar chimney and wind energy for hybrid desalination via reverse osmosis and multi-stage flash with brine recovery," vol. 44, no. 2020, 2021, doi: 10.1016/j.seta.2021.101080.

[125] M. Tawalbeh, S. Mohammed, A. Alnaqbi, S. Alshehhi, A. Al-Othman, Analysis for hybrid photovoltaic/solar chimney seawater desalination plant: a CFD simulation in Sharjah, United Arab Emirates, Renew. Energy 202 (2023) 667–685, https://doi.org/10.1016/j.renene.2022.11.106.

[126] E. Abdelsalam, F. Kafiah, M. Alkasrawi, I. Al-Hinti, A. Azzam, Economic study of solar chimney power-water distillation plant (SCPWDP), Energies. (Basel) 13 (11) (2020), https://doi.org/10.3390/en13112789.

[127] M. Abedi, X. Tan, J.F. Klausner, A. Bénard, Solar desalination chimneys: investigation on the feasibility of integrating solar chimneys with humidification–dehumidification systems, Renew. Energy 202 (2023) 88–102, https://doi.org/10.1016/j.renene.2022.11.069.

[128] L. Zuo, C. Xiao, Z. Yan, Z. Guo, L. Huang, Y. Ge, Experimental and simulation study on the performance of corrugated plate enhanced solar chimney power plant combined with distillation system, Desalination. 600 (2025) 118534, https://doi.org/10.1016/j.desal.2025.118534.

[129] E. Abdelsalam, et al., A case study of an integrated solar chimney power plant and water desalination plant in Qatar, Desalination. 575 (2024) 117283, https://doi.org/10.1016/j.desal.2023.117283.

[130] L. Zuo, L. Huang, Z. Yan, C. Xiao, Z. Guo, Y. Ge, Analysis of characteristics of seawater desalination-solar chimney power plant under double-layer collector, Appl. Therm. Eng. 257 (2024) 124274, https://doi.org/10.1016/j.applthermaleng.2024.124274.

[131] A. Mebarki, A. Sekhri, A. Assassi, A. Hanafi, CFD analysis of solar chimney power plant: finding a relationship between model minimization and its performance for use in urban areas, Energy Reports 8 (2022) 500–513, https://doi.org/10.1016/j.egyr.2021.12.008.

[132] M. Saad, N. Ahmed, L. Giovannini, M. Mahmood, M.U. Rafi, M.A. Qaisrani, Evaluation of possible integration of solar chimney power plants with high-rise buildings: a numerical analysis, J. Build. Eng. 60 (August) (2022) 105188, https://doi.org/10.1016/j.jobe.2022.105188.

[133] M.H. Titi, A. Mebarki, A. Assassi, Integration of the Manzanares solar chimney power plants in towers: collector and building height configuration, Eng., Technol. Appl. Sci. Res. 15 (3) (2025) 23002–23007, https://doi.org/10.48084/etasr.10594.

[134] S. Fereidoni, L. Fereidooni, S.T. Shabestari, M.S. Esmaeili, M. Zare, A. Kasaeian, Application of solar chimneys and hybrid solar chimneys for ventilation in buildings: a review, Solar Energy 288 (113246) (2025), https://doi.org/10.1016/j.solener.2025.113246. Art. no.

[135] A. Dhahri, A. Omri, and J. Orfi, "Theoretical analysis of the performance of a solar chimney coupled with a geothermal heat exchanger BT - CFD techniques and energy applications," Z. Driss, B. Necib, and H.-C. Zhang, Eds. Cham: Springer International Publishing, 2018, pp. 1–27, https://doi.org/10.1007/978-3-319-70950-5_1.

[136] F. Cao, H. Li, Q. Ma, L. Zhao, Design and simulation of a geothermal–solar combined chimney power plant, Energy Convers. Manage 84 (2014) 186–195, https://doi.org/10.1016/j.enconman.2014.04.015.

[137] Z. Zou, S. He, Modeling and characteristics analysis of hybrid cooling-tower-solar-chimney system, Energy Convers. Manage 95 (2015) 59–68, https://doi.org/10.1016/j.enconman.2015.01.085.

[138] O.B.E.K. Mokrani, M.R. Ouahrani, M.H. Sellami, L. Segni, Experimental investigations of hybrid: geothermal water/solar chimney power plant, Energy Sources, Part A Recover. Util. Environ. Eff. (2020) 1–18, https://doi.org/10.1080/15567036.2020.1810830. Aug.

[139] A. Habibollahzade, E. Houshfar, M. Ashjaee, K. Ekradi, Continuous power generation through a novel solar /geothermal chimney system: technical / cost analyses and multi-objective particle swarm optimization, J. Clean. Prod. 283 (2021) 124666, https://doi.org/10.1016/j.jclepro.2020.124666.

[140] M.H. Haji, Molla Ali Tork, E. Houshfar, M. Ashjaee, Integrating geothermal energy and a solar chimney to maximize renewable energy production: an analytical investigation of a novel hybrid system, Renew. Energy 230 (2024) 120827, https://doi.org/10.1016/j.renene.2024.120827.

[141] N. Fathi, P. McDaniel, P. Vorobieff, C. de Oliveira, S. Rodriguez, and S.S. Aleyasin, "Thermal-CFD analysis of combined solar-nuclear cycle systems," 2015, https://www.osti.gov/servlets/purl/1427233.

[142] K.R. Anderson, M. Shafahi, C. McNamara, Thermal-fluids analysis of a hybrid solar/compost waste heat updraft tower, J. Clean Energy Technol. 4 (3) (2015) 213–220, https://doi.org/10.7763/jocet.2016.v4.283.

[143] K.R. Anderson, et al., Design of a compost waste heat to energy solar Chimney Power plant, J. Civ. Eng. Res. 6 (3) (2016) 47–54, https://doi.org/10.5923/j.jce.20160603.01, 2016.

[144] K.R. Anderson, M. Shafahi, R.B. Lakeh, S. Monmeni, C. McNamara, CFD analysis of hybrid solar tower using compost waste heat and photovoltaics, in: Proceedings of the IEEE SUSTECH 2015 Conference on Technologies and Sustainability, Ogden, Utah, USA, 2015.

[145] H.H.Al-Kayiem Azeemuddin, S.I. Gilani, Simulation of a collector using waste heat energy in a solar chimney power plant system, WIT Trans. Ecol. Environ. 179 (VOLUME) (2013) 933–944, https://doi.org/10.2495/SC130792.

[146] H.H. Al-Kayiem, K. Yin Yin, C.Yee Sing, Numerical simulation of solar chimney integrated with exhaust of thermal power plant, WIT Trans. Eng. Sci. 75 (2012) 61–72, https://doi.org/10.2495/HT120061.

[147] A. Zandian, M. Ashjaee, The thermal efficiency improvement of a steam Rankine cycle by innovative design of a hybrid cooling tower and a solar chimney concept, Renew. Energy 51 (2013) 465–473, https://doi.org/10.1016/j.renene.2012.09.051.

[148] B. Ghorbani, M. Ghashami, M. Ashjaee, Electricity production with low grade heat in thermal power plants by design improvement of a hybrid dry cooling tower and a solar chimney concept, Energy Convers. Manage 94 (2015) 1–11, https://doi.org/10.1016/j.enconman.2015.01.044.

[149] S. Hu, D.Y.C. Leung, Numerical modelling of the compressible airflow in a solar-waste-heat chimney power plant, Energy Procedia 142 (2017) 642–647, https://doi.org/10.1016/j.egypro.2017.12.106.

[150] M.A. Aurybi, H.H. Al-Kayiem, S.I.U. Gilani, A.A. Ismaeel, CFD analysis of hybrid Solar Chimney Power Plant, in: MATEC Web of Conferences 225, 2018, https://doi.org/10.1051/matecconf/201822504011.

[151] M.M. Esmaili, S.H. Fallah, M. Izanlu, S. Valipour, Investigation on the performance of a solar chimney-flare gas hybrid system, Sustain. Energy Technol. Assessm. 52 (2022) 102279, https://doi.org/10.1016/j.seta.2022.102279. PC.

[152] P.M. Cuce, E. Cuce, S. Omer, S. Riffat, Solar chimney power plant with integrated waste heat source on the ground: a numerical and statistical research with experimental validation, Int. J. Low-Carbon Technol. 20 (2025) 1272–1282, https://doi.org/10.1093/ijlct/ctaf077.

[153] E. Abdelsalam, F. Almomani, F. Kafiah, H. Alnawafah, A. Juaidi, R. Abdallah, Integrating solar chimney power plant with electrolysis station for green hydrogen production: a promising technique, Int. J. Hydrogen. Energy 52 (2024) 1550–1563, https://doi.org/10.1016/j.ijhydene.2023.08.305.

[154] O.J. Shariatzadeh, A.H. Refahi, S.S. Abolhassani, M. Rahmani, Modeling and optimization of a novel solar chimney cogeneration power plant combined with solid oxide electrolysis/fuel cell, Energy Convers. Manage 105 (2015) 423–432, https://doi.org/10.1016/j.enconman.2015.07.054.

[155] X. Fei, R. Xuejun, N. Razmjooy, Optimal configuration and energy management for combined solar chimney, solid oxide electrolysis, and fuel cell: a case study in Iran, Energy Sources, Part A Recover. Util. Environ. Eff. 45 (4) (Oct. 2023) 9794–9814, https://doi.org/10.1080/15567036.2019.1680770.

[156] A. Jemal, Z. Yahya, O. Drame, A.M. Mahmoud, A. Alhodaib, V. Ali, O. Khan, A. K. Yadav, Optimization of hybrid solar chimney power plant using Pearson and k-means analysis for green hydrogen and electricity production, Sci. Rep. 15 (40729) (2025), https://doi.org/10.1038/s41598-025-24507-5. Art. no.

[157] R. Škoda et al., "TEPLATOR: nuclear district heating solution," 2020, doi: http://hdl.handle.net/11025/42640.

[158] H.A.S. Abushamah, D. Masata, M. Mueller, R. Skoda, Economics of reusing spent nuclear fuel by Teplator for district heating applications, Int. J. Energy Res. 46 (5) (Apr. 2022) 5771–5788, https://doi.org/10.1002/er.7521.

[159] J. Li, P. Guo, Y. Wang, Effects of collector radius and chimney height on power output of a solar chimney power plant with turbines, Renew. Energy 47 (2012) 21–28, https://doi.org/10.1016/j.renene.2012.03.018.

[160] N. Fathi, S.S. Aleyasin, P. Vorobieff, Numerical-analytical assessment on Manzanares prototype, Appl. Therm. Eng. 102 (2016) 243–250, https://doi.org/10.1016/j.applthermaleng.2016.03.133.

[161] A. Koonsrisuk, T. Chitsomboon, Mathematical modeling of solar chimney power plants, Energy 51 (2013) 314–322, https://doi.org/10.1016/j.energy.2012.10.038.

[162] P. Guo, Y. Wang, J. Li, Y. Wang, Thermodynamic analysis of a solar chimney power plant system with soil heat storage, Appl. Therm. Eng. 100 (2016) 1076–1084, https://doi.org/10.1016/j.applthermaleng.2016.03.008.

[163] Y.J. Choi, D.H. Kam, Y.W. Park, Y.H. Jeong, Development of analytical model for solar chimney power plant with and without water storage system, Energy 112 (2016) 200–207, https://doi.org/10.1016/j.energy.2016.06.023.

[164] E. Gholamalizadeh, J.D. Chung, A comparative study of CFD models of a real wind turbine in solar chimney power plants, Energies. (Basel) 10 (10) (2017), https://doi.org/10.3390/en10101674.

[165] J.D. Anderson, Governing equations of fluid dynamics, Comput. Fluid Dyn. (1992) 15–51, https://doi.org/10.1007/978-3-540-85056-4_2.

[166] E. Gholamalizadeh, M.-H. Kim, Three-dimensional CFD analysis for simulating the greenhouse effect in solar chimney power plants using a two-band radiation model, Renew. Energy 63 (2014) 498–506, https://doi.org/10.1016/j.renene.2013.10.011.

[167] W. Ye, et al., Chapter 3 - design with modeling techniques, in: Second E. Wang (Ed.), H. D. Goodfellow and Y. B. T.-I. V. D. G., Academic Press, 2021, pp. 109–183, https://doi.org/10.1016/B978-0-12-816673-4.00008-0.

[168] J. Schlaich, R. Bergermann, W. Schiel, G. Weinrebe, Sustainable electricity generation with solar updraft towers, Struct. Eng. Int.: J. Int. Assoc. Bridge Struct. Eng. (IABSE) 14 (3) (2004) 225–229, https://doi.org/10.2749/101686604777963883.

[169] X. Zhou, J. Yang, A novel solar thermal power plant with floating chimney stiffened onto a mountainside and potential of the power generation in China's deserts, Heat Transf. Eng. 30 (5) (2009) 400–407, https://doi.org/10.1080/01457630802414813.

[170] T.P. Fluri, J.P. Pretorius, C. Van Dyk, T.W. Von Backström, D.G. Kröger, G.P.A.G. V. Zijl, Cost analysis of solar chimney power plants, Sol. Energy 83 (2) (2009) 246–256, https://doi.org/10.1016/j.solener.2008.07.020.

[171] F. Cao, H. Li, L. Zhao, L. Guo, Economic analysis of solar chimney power plants in Northwest China, J. Renew. Sustain. Energy 5 (2) (2013), https://doi.org/10.1063/1.4798434.

[172] W. Li, P. Wei, X. Zhou, A cost-benefit analysis of power generation from commercial reinforced concrete solar chimney power plant, Energy Convers. Manage 79 (2014) 104–113, https://doi.org/10.1016/j.enconman.2013.11.046.

[173] L. Zuo, et al., Performance study and economic analysis of wind supercharged solar chimney power plant, Renew. Energy 156 (2020) 837–850, https://doi.org/10.1016/j.renene.2020.04.032.

[174] M.A. Aziz Bhuiyan, M.H. Bhuiyan, M.A. Rahman, M.A. Abir, N. Mehfuz, S. Salehin, Economic assessment of concrete and floating based solar chimney power plants in Bangladesh, 2020 IEEE Region 10 Symposium, TENSYMP 2020 (2020) 638–641, https://doi.org/10.1109/TENSYMP50017.2020.9230846.

[175] B. Van Blommestein and C. Mbohwa, "Life cycle assessment of solar chimneys BT - re-engineering manufacturing for sustainability," 2013, pp. 535–541, https://doi.org/10.1007/978-981-4451-48-2_87.

[176] T. Salameh, et al., Economic and environmental assessment of the implementation of solar chimney plant for water production in two cities in UAE, Therm. Sci. Eng. Prog. 33 (March) (2022) 101365, https://doi.org/10.1016/j.tsep.2022.101365.

[177] J. Pretorius, Optimization and Control of a Large-Scale Solar Chimney Power Plant, University of Stellenbosch, 2007.

[178] Y. Xu, X. Zhou, Performance of a modified solar chimney power plant for power generation and vegetation, Energy 171 (2019) 502–509, https://doi.org/10.1016/j.energy.2019.01.033.

[179] A.A. Hachicha, E.M. Abo-Zahhad, M. Masmoudi, Z. Said, S.M.A. Rahman, Techno-economic evaluation and multi-objective optimization of a filter equipped solar chimney system, Renew. Energy 237 (2024) 121452, https://doi.org/10.1016/j.renene.2024.121452.

[180] H.A.S. Abushamah, D. Masata, J. Jiřičková, and R. Škoda, "Optimization of sizing and operation of a nuclear district heating system using Teplator, gas boiler and heat storage," 2022, https://www.djs.si/nene2022/proceedings/htm/pdf/NENE2022_910.pdf?utm.

[181] Y. Tian, C.Y. Zhao, A review of solar collectors and thermal energy storage in solar thermal applications, Appl. Energy 104 (104) (Apr. 2013) 538–553, https://doi.org/10.1016/j.apenergy.2012.11.051.

[182] S.A. Kalogirou, *Solar thermal collectors and applications*, vol. 30, no. 3. 2004, https://doi.org/10.1016/j.pecs.2004.02.001.

[183] H.H. Al-kayiem, M.A. Aurybi, and S.I.U. Gilani, "Influence of canopy condensate fi lm on the performance of solar chimney power plant," vol. 136, pp. 1012–1021, 2019, doi: 10.1016/j.renene.2019.01.067.

[184] R. Mehdipour, Z. Baniamerian, S. Golzardi, S.M.S. Murshed, Geometry modification of solar collector to improve performance of solar chimneys, Renew. Energy 162 (2020) 160–170, https://doi.org/10.1016/j.renene.2020.07.151.

[185] Y. Sheikhnejad, S. Abdolreza, G. Nassab, Enhancement of solar chimney performance by passive vortex generator, Renew. Energy 169 (2021) 437–450, https://doi.org/10.1016/j.renene.2021.01.026.

[186] D. Toghraie, A. Karami, M. Afrand, A. Karimipour, Effects of geometric parameters on the performance of solar chimney power plants, Energy 162 (2018) 1052–1061, https://doi.org/10.1016/j.energy.2018.08.086.

[187] F. Cao, T. Yang, Q. Liu, T. Zhu, H. Li, L. Zhao, Design and simulation of a solar double-chimney power plant, Renew. Energy 113 (2017) 764–773, https://doi.org/10.1016/j.renene.2017.05.100.

[188] M.A. Aziz, A.M. Elsayed, Thermofluid effects of solar chimney geometry on performance parameters, Renew. Energy 200 (October) (2022) 674–693, https://doi.org/10.1016/j.renene.2022.10.022.

[189] E. Cuce, P.M. Cuce, H. Sen, K. Sudhakar, U. Berardi, U. Serencam, Impacts of ground slope on main performance figures of solar chimney power plants: a comprehensive CFD research with experimental validation, Int. J. Photoenergy 2021 (2021), https://doi.org/10.1155/2021/6612222.

[190] H. Nasraoui, Z. Driss, H. Kchaou, Novel collector design for enhancing the performance of solar chimney power plant, Renew. Energy 145 (2020) 1658–1671, https://doi.org/10.1016/j.renene.2019.07.062.

[191] E. Abdelsalam, et al., An innovative design of a solar double-chimney power plant for electricity generation, Energies. (Basel) 14 (19) (2021), https://doi.org/10.3390/en14196235.

[192] T. Singh, A. Kumar, Numerical analysis of the divergent solar chimney power plant with a novel arc and fillet radius at the chimney base region, Renew. Energy 228 (2024) 120504, https://doi.org/10.1016/j.renene.2024.120504.

[193] H. Xiong, et al., Numerical investigation on performance of solar chimney power plant with three wind resistant structures, Energy 297 (2024) 131262, https://doi.org/10.1016/j.energy.2024.131262.

[194] D. Kumar Mandal, N. Biswas, N.K. Manna, A.C. Benim, Impact of chimney divergence and sloped absorber on energy efficacy of a solar chimney power plant (SCPP), Ain Shams Eng. J. 15 (2) (2024) 102390, https://doi.org/10.1016/j.asej.2023.102390.

[195] D.K. Mandal, N. Biswas, N.K. Manna, D.K. Gayen, A.C. Benim, Sustainable design of solar chimney power plants: a hybrid neural network approach for thermo-economic optimization, Renew Energy 256 (2025) 124154, https://doi.org/10.1016/j.renene.2025.124154.